PATTERN OF SEROTONERGIC INNERVATION TO INTRINSIC AND OUTPUT NEURONS IN THE CAT NEOSTRIATUM

Tetsu OKUMURA

Doctor of Philosophy

Department of Physiological Sciences,

School of Life Sciences,

The Graduate University for Advanced Studies

and

Department of Biological Control System,

National Institute for Physiological Sciences,

Myodaiji, Okazaki, 444-8585

JAPAN

1999

CONTENTS

Part 1 Relative distribution of cholinergic neurons vs. serotonergic fibers in the cat neostriatum

ABSTRACT ... 2

INTRODUCTION ... 3

MATERIALS AND METHODS ... 5

Choline-acetyltransferase immunohistochemistry ... 5

5-HT immunohistochemistry ... 5

Observations and analyses ... 6

RESULTS ... 7

Distribution and morphology of ChAT-immunopositive cells in the neostriatum ... 7

Distribution of 5-HT-immunopositive fiber in the neostriatum ... 9

DISCUSSION ... 12

The cholinergic system of the neostriatum ... 12

Serotonergic innervation of the neostriatum ... 13

Functional implication of cholinergic and serotonergic Innervation ... 15

REFERENCES ... 16

FIGURE LEGENDS 22

Figure 1-5

Part 2 Distribution and fine morphology of neostriatal output neurons, and serotonergic innervation to the output neurons and cholinergic interneurons in the cat

ABSTRACT 2

INTRODUCTION 3

MATERIALS AND METHODS 6

Labeling of the neostriatal output cells and 5-HT fibers 6

Labeling of cholinergic interneurons and 5-HT fibers 8

Analyses 9

RESULTS 11

Distribution of the neostriatal output cells projecting to the GP, EP and SNR and their morphology 11

5-HT innervation to the neostriatal output cells and cholinergic interneurons 15

DISCUSSION 18

Topographical organization of striatal projection neurons

to the GP, EP and SNR 18

Serotonergic innervation to the output neurons and interneurons

in the neostriatum 20

Functional role of the srotonergic innervation of Cholinergic

interneurons and output projections neurons 21

REFERENCES 25

FIGURE LEGENDS 33

Figure 1-10

ACKNOWLEDGEMENTS

Part 1

Relative distribution of cholinergic neurons vs. serotonergic fibers in the cat neostriatum

Tetsu OKUMURA

Doctor of Philosophy

Department of Physiological Sciences,

School of Life Sciences,

The Graduate University for Advanced Studies

and

Department of Biological Control System,

National Institute for Physiological Sciences,

Myodaiji, Okazaki, 444-8585

JAPAN

Number of text pages: 23 (including a title page)

Number of figures: 5

ABSTRACT

The distribution of choline acetyltransferase (ChAT)-containing neurons and serotonin (5-HT)-containing nerve fibers in the cat neostriatum was investigated by use of immunohistochemical techniques. Both ChAT- and 5-HT-staining techniques were applied to alternate brain sections, thereby allowing a precise comparison of the distribution pattern of ChAT-immunopositive cells (ChAT cells) and 5-HT-immunopositive fibers (5-HT fibers). In the neostriatum, ChAT cells were strongly stained throughout their cell bodies and proximal (1st-order) dendrites. The majority of them were multipolar cells with a soma diameter of 20-50 μm (long axis) X 10-30 μm (short axis). In the caudate nucleus, ChAT cells were evenly and diffusely distributed except for the dorsolateral region of its rostral half, in which latter region they were distributed in loosely formed clusters. In the rostral portion of the putamen, the density of ChAT-cell distribution was like that in the medial region of the caudate nucleus. In contrast, this distribution was more dense in the caudomedial region of the putamen, adjacent to the globus pallidus. 5-HT fibers in the neostriatum were dark-stained, of quite fine diameter (< 0.6 μm), and they contained small, round varicosities (diameter, usually 0.5-1.0 μm, but some >1.0 μm). Such 5-HT fibers were distributed abundantly throughout the caudate nucleus and putamen. In the rostrocaudal portion of the caudate nucleus, their density was high in its dorsal and ventral components, and low in the middle component. Throughout the putamen, 5-HT fibers were distributed homogeneously in the mediolateral and dorsoventral directions. In the caudal portion of the putamen adjacent to the globus pallidus, the 5-HT fibers had a higher density while maintaining their homogenous distribution pattern. In the two main divisions of the striatum, the so-called "patch" (AchE-poor) and "matrix" (AchE-rich) compartments, there was a near-even distribution of 5-HT fibers and terminals. The above results suggest that the 5-HT-dominated, raphe-striatal pathway is optimally arranged for modulating the activity of both the intrinsic and the projection neurons of the neostriatum.

INTRODUCTION

In vertebrates, the principal component of the basal ganglia is the striatum. It consists of the caudate, putamen, and accumbens nuclei. The predominant cell type among the striatum's neurons is the medium-sized spiny cell (80-84% with a soma diameter of 10-20 μm) that uses GABA as its primary transmitter (Kita and Kitai, 1988). It accounts for 90-95% of the striatum's total neuronal population, by far the majority of which (~ 90%) are projection cells whose axons exit from the striatum. Converging on the striatal spiny GABAergic projection cells are at least: 1) cortical glutamatergic excitatory inputs; 2) mesencephalic dopaminergic (DA) inhibitory inputs; 3) inputs from the local axon collaterals of other spiny projection cells and/or inputs from intrinsic neurons (Wilson and Groves, 1980); and 4) serotonergic projections from the dorsal raphe nucleus, as demonstrated in the rat and cat (Sano et al., 1982; Steinbusch et al., 1978, 1981).

About 10% of the striatum's total cell population are intrinsic neurons, whose axons do not exit the striatum (Gerfen, 1992). About 20 % of this intrinsic group comprise another striatum's cell type, the large-sized (soma diameter, 20-50 μm [long axis] X 10-30 μm [short axis]), aspiny cell that uses acetylcholine (Ach) as its transmitter (Bolam et al., 1984). This latter population is the focus of the present study.

The striatum is a heterogeneous structure in which two divisions (compartments) have been distinguished on the basis of their acetylcholinesterase (AchE) representation (Graybiel and Ragsdale, 1978; Graybiel et al., 1986). Within the striatum, there are patches which are AchE-poor, whereas the overall matrix is AchE-rich (Desban et al., 1989). Hence, the now-popular terminology: the patch and matrix compartments of the striatum. In both the rat and cat, these compartments also differ by virtue of the different input- and output-projection patterns of their DA neurons (Gerfen et al., 1987; Jimenez-Castellanos and Graybiel, 1987).

Within the matrix component of the striatum, mapping studies, using either AchE or choline acetyltransferase (ChAT), have indicated that cholinergic cells are scattered throughout the full extent of the caudate nucleus and putamen. These

neurons have been estimated to be < 5% of the total striatal population in the rat (Kemp and Powell, 1971) and even less (1-2%) in the cat (Phelps et al., 1985). Striatal intrinsic cholinergic neurons are critically involved in the dopaminergic modulation of striatal projection neurons, thereby exerting profound effects on the overall control of behavior (Gerfen, 1992).

As part of our laboratory's multi-pronged attempt to understand the functional role played by the striatal cholinergic system in behavioral control, we have recently perfused the caudate nucleus with artificial cerebrospinal fluid containing a high concentration of cholinergic agonists. This was accomplished in the conscious, unrestrained, intact cat by means of a microdialysis technique (Kekesi et al., 1997; Okumura et al., 1998). Perfusion of the caudate nucleus for ~ 40 min with carbachol, a cholinergic agonist resistant to hydrolysis by AchE, produced arousal reactions in the animal, which began ~ 30 min into the perfusion, and continued for several hours. These reactions were accompanied by hyperreactive responses to external stimuli. During the first 2 hr of this period of altered behavior, the extracellular level of serotonin (5-HT) in the caudate nucleus was increased significantly, with the peak level occurring at ~ 1 hr.

The above finding led to the present study, in which ChAT-immunohistochemistry (Cote et al., 1993) was used to reexamine the distribution of ChAT-containing cells in the cat neostriatum, including its caudate nucleus component. The distribution of 5-HT-containing fibers in the caudate nucleus was also studied, by use of 5-HT-immunohistochemistry (Sano et al., 1982; Kobayashi et al., 1994; Tanaka et al., 1992). The latter measurements were made on single serial sections adjacent to those labeled for ChAT.

Some of the present results have been presented previously in abstract (Okumura et al., 1999).

MATERIALS AND METHODS

Experiments were performed on 6 adult cats of either sex (2 male; 4 female) weighing 2.2-4.2 kg. They were deeply anesthetized with pentobarbital (40 mg/kg, i.p.) and perfused transcardially: first, for 20-30 min with 0.01M phosphate-buffered saline (PBS, 1 l/kg) to wash out the blood; and, subsequently, for 20-30 min with a chilled (4 °C) fixative containing 4 % paraformaldehyde, 0.35 % glutaraldehyde and 0.2 % picric acid in 0.1 M phosphate buffer (pH 7.4, 1 l/kg). After the perfusion, the brain, including the brainstem, was removed immediately and post-fixed for 2 days at 4 °C in a fixative containing 4 % paraformaldehyde and 0.2 % picric acid in 0.1 M phosphate buffer. The tissue was then immersed in 0.1 M phosphate buffer containing 20 % sucrose for at least another 2 days at 4 °C. Transverse serial sections of the forebrain and brainstem were cut on a cryotome at a thickness of 50 μm.

Choline-acetyltransferase immunohistochemistry

Every 4th serial section of the forebrain including the neostriatum, was used for determination of the distribution of ChAT-containing cells. These sections, in a free-floating state, were incubated for 2 days at 4 °C with monoclonal ChAT antibody from rat/mouse hybrid cells (diluted to 0.33 μg antibody/ml; Boehringer Mannheim Bio, Germany) at room temperature (20-25° C), and then incubated: first, with biotinylated-rabbit anti-rat IgG for 1hr; and second, with avidin-biotin-peroxidase complex for 1 hr. Finally, the sections were reacted with 0.06% 3,3'-diaminobendizine (DAB) and 0.01% H_2O_2 in 0.01M Tris-HCl buffer for 5-15 min (Cote et al., 1993). After immunostaining, the sections were mounted onto gelatin-coated glass slides, dehydrated, and cover-slipped.

5-HT immunohistochemistry

Every 4th serial section immediately adjacent to those used for ChAT-immunohistochemistry was utilized for determination of the distribution of 5-HT-containing nerve fibers. These sections, also in a free-floating state, were incubated for 2 days at room temperature with rabbit 5-HT antiserum (diluted 1:20,000), followed by incubations with: first, biotinylated goat anti-rabbit IgG for 2 hr; and second,

avidin-biotin-peroxidase complex for 1 hr. Finally, the sections were reacted with 0.01% DAB, 1% nickel ammonium sulfate and 0.0003% H_2O_2 in 0.05M Tris-HCl buffer for at least 20 min (Takeuchi et al., 1982). After immunostaining, the sections were mounted onto gelatin-coated glass slides, dehydrated and cover-slipped. Some sections were lightly counterstained with 1 % neutral red.

Observations and analyses

All stained sections were examined under a light microscope equipped with a light-field condenser. The locations of ChAT-immunopositive cells observed in the neostriatum and its surrounding region were carefully plotted from each transverse section, using a camera lucida. 5-HT-immunopositive fibers located in the caudate nucleus and putamen of representative sections were treated similarly. The camera lucida drawings were made with a X20 dry objective, and the final magnification of drawings was at X200. The diameter of ChAT-positive cells and 5-HT-positive terminal boutons were measured at high power (X1000) under a X100 oil-immersion objective. In these measurements, no correction was made for possible shrinkage of axons as a result of the histological procedures (Grace and Llinas, 1985). The perikaryal areas of ChAT-positive cells in the caudate nucleus, putamen and globus pallidus (GP) were also measured, using the public domain NIH Image Program (U.S. National Institutes of Health) on a Macintosh computer.

Photomicrographs were taken with a conventional 35-mm film camera connected to the microscope, and then scanned to make figures. Some photomicrographs (e.g., Figure 2) were taken with a Polaroid digital microscope camera (resolution: 1600 x 1200 pixels) connected to the same microscope. The luminosity of the raw photomicrographs was modified by use of graphics software on a PC computer. The illustration plates were printed with a digital color printer (Pictrography 3000, Fujifilm Co, Japan).

Anatomical nomenclature conforms to the description of Berman and Jones (1982).

RESULTS

A key feature of the present study was that the distribution pattern of cholinergic neurons vs. serotonergic fibers was compared *precisely* in the neostriatum of the *same* animals by applying ChAT- and 5-HT-immunohistochemistry to *immediately adjacent* serial sections. This provided the means to characterize the region-specific innervation pattern of cholinergic vs. serotonergic systems in the neostriatum.

Distribution and morphology of ChAT-immunopositive cells in the neostriatum

In ChAT-immunostained sections, we found that most of ChAT-immunopositive cells (ChAT cells) were strongly stained throughout the soma and the proximal dendrites (at least 200 μm deep into the latter). The stained cells were multipolar with a soma diameter of 20-50 μm (long axis) X 10-30 μm (short axis). They were distributed throughout the full rostral to caudal extent of the neostriatum (i.e., Horsley-Clarke co-ordinate, A20.0-11.5).

Figure 1 shows the distribution of ChAT cells, irrespective of their size and shape, in 8 transverse planes from A19.3 to A12.7. Throughout the caudate nucleus, their density was ~ 7-10 cells/mm^2. In the medial region of the rostral (A19.3-16.4) and caudal (A15.5-12.7) halves of the nucleus, the cells were distributed evenly and diffusely. In contrast, in the dorsolateral region, they were distributed in contiguous groups, thereby forming loose clusters surrounded by relatively extensive ChAT-cell-free areas.

In the rostral putamen (A19.3-18.3), the ChAT cells had a lower density (approximately 5 cells/mm^2) vs. that in the caudate nucleus. At the caudal level (A17.4-12.7) of the putamen, however, their density was increased remarkably (13, 20 and 24 cells/ mm^2 at levels A17.4, 15.5 and 12.7, respectively). At A15.5-12.7, in particular, the ChAT cells were much more densely distributed in the medial region of the putamen, immediately adjacent to the globus pallidus.

In addition to the caudate nucleus and putamen, many of the ChAT cells were distributed in the internal capsule at A16.4-13.7. These cells were diffusely scattered in the ventral region, while those in the dorsal region were located in strips coursing

between the caudate nucleus and putamen (see A15.5-13.7 in Fig. 1).

Figure 2 provides low- and high-magnification photomicrographs of the morphological features of ChAT cells, as observed in the caudate nucleus (A, D), the putamen and globus pallidus (B and E, respectively), and ChAT-immunostained strips in the internal capsule (C, F). (The locations at which photomicrographs A, B and C were taken are indicated by squares in the Figure 1 drawings at A18.3, 15.5 and 13.7, respectively).

In the caudate nucleus (Fig. 2, A and D), the majority of the ChAT cells were multipolar in shape, the remaining being fusiform or pyramidal. Multipolar cells had 3–6 proximal (1st-order) dendrites, whereas fusiform and pyramidal cells had 2-3. None of the ChAT cells had spine-like structures on their dendrites. Therefore, they were all classified as aspiny neurons. The range of soma diameters for the caudate ChAT cells along their long X short axis was 18-50 X 8-31 μm. Their mean ± SEM perikaryal area was 349 ± 6.9 μm^2 (n=240). The labeled caudate cells in Figure 2 (A and D) were a multipolar one, with 5 proximal dendrites, and a pyramidal one, with 3 proximal dendrites. Since no ChAT-positive terminal boutons were found on the surface of the soma and proximal dendrites, the caudate ChAT cells appeared to be purely cholinergic.

In the putamen, the majority of the ChAT cells were multipolar in shape. In the rostral one third of this structure, their soma-diameter range was 21-50 X 10-27 μm, like that in the caudate nucleus. In the caudal two-thirds of the putamen, we found larger-sized multipolar cells with a soma-diameter range of 24-52 X 12-37 μm. The mean perikaryal area of ChAT cells in the rostral vs. caudal putamen (n=40 in each region) was 382.8 ± 17.0 vs. 450.3 ± 13.9 μm^2. The multipolar putamen cell in Figure 2B had a soma diameter of 35 μm (long-axis) and 5 proximal dendrites.

In the globus pallidus, large-sized aspiny neurons with a soma-diameter range of 27-66 X 12-33 μm were aggregated densely. The mean perikaryal area of pallidal ChAT cells was 553.8 ± 16.9 μm^2 (n=60). In this nucleus, the region around ChAT cells was stained (albeit weakly), thereby permitting the visualization of a cholinergic neuropil including terminal boutons around the pallidal ChAT cells. In some cases,

ChAT-positive terminal boutons were closely apposed to the soma and proximal dendrites (e.g., see Fig. 2E), indicating that such cells are presumably cholinoceptive-cholinergic neurons. One such pallidal cell is shown in Figure 2E. It was a large pyramidal one with 3 proximal dendrites.

In the internal capsule, Figure 2C shows that ChAT-immunostained strips could be observed to help form a bridge between the caudate nucleus and the putamen. ChAT-positive cells were located in these strips, together with bundles of ChAT-positive neuropils. A majority of the internal capsule's ChAT cells were of fusiform shape with a soma-diameter range of 30-50 X 15-25 μm (e.g., as in Fig. 2F). The long axes of their somas were directed parallel to the course of the bundles of labeled fibers.

Figure 3 provides low-magnification photographs of the overall neostriatum, using ChAT-immunostained sections at A18.3, 16.4 and 14.5, respectively. These sections were adjacent to those used for analysis of the distribution of ChAT cells shown in Figure 1. They were immunoreacted intensely, in order to obtain a high background staining of the neostriatum. In the Figure 3 sections, heterogeneous staining was observed throughout the neostriatum, particularly in the caudate nucleus, with scattered, lightly stained regions interposed among intensely stained regions. This heterogeneity was most prominent in the anterior half of the caudate nucleus (i.e., A18.3 and 16.4 in Fig. 3). It is likely that these lightly and intensely stained regions corresponded to the patches and matrix organization of the striatum, respectively (cf. Graybiel and Ragsdale, 1978).

Distribution of 5-HT-immunopositive fibers in the neostriatum

In Figure 4A, the three low-magnification photographs of 5-HT-immunopositive fibers (5-HT fibers) were taken from transverse serial sections at striatal levels, A18.3, 16.4, and 14.5. These sections were immediately adjacent to those shown above in Figure 3.

Figure 4B-C shows that the stained 5-HT fibers were distributed profusely throughout the caudate nucleus (B), and the putamen (C). Such distribution was also observed in the globus pallidus and substantia innominata (e.g., Fig. 4A, A14.5, lowest

quarter; dense distribution also seen in remaining components of these two structures).

Region-specific, 5-HT-immunostaining patterns were evident within the caudate nucleus and the putamen. For example, throughout the rostrocaudal extent of the caudate nucleus, the intensity of 5-HT staining was high in the dorsal (Fig. 4A, A18.3, top part of nucleus) and ventral (Fig. 4Bc, lower-right quadrant) portions of the nucleus, whereas such staining was relatively low in the middle portion (Fig. 4Bb, mid-right area). In the caudate nucleus, we did not observe a patch and matrix distribution of 5-HT staining, like the ChAT-immunostaining, shown above in Figure 3.

At each level tested in the putamen (e.g., Fig. 4C), 5-HT immunostaining was relatively homogeneous in the mediolateral and dorsoventral directions. At more caudal levels adjacent to the globus pallidus (Fig. 4C, A14.5, lower-right quadrant), the intensity of 5-HT staining increased, with retention of the homogenous distribution pattern.

Usually, the 5-HT fibers did not form compact and distinct fiber bundles in the striatum, such as occurs in the pyramidal tract. In the caudate nucleus (Fig. 5A-B), there were few fiber-free areas. Most of the caudate 5-HT fibers were of fine diameter (~ 0.6 μm) with small varicosities (diameter, usually 0.5-1.0 μm, but some >1.0 μm). These fine fibers formed mesh-like plexuses. In addition, a few fibers with larger varicosities (diameter, 1.5-2.0 μm) were distributed sparsely throughout this nucleus. The fibers with small vs. large varicosities corresponded to the C- vs. B-fibers, respectively, of the Sano et al. (1982) classification scheme.

In the putamen (Fig. 5C), most of the 5-HT fibers were like the majority of the caudate ones (i.e., they were C-fibers) and, again, they formed mesh-like plexuses. A small number of putamen B-fibers were also present, but they were distributed quite sparsely. In addition, dorsally running, thick (diameter, ~ 1.0 μm) *smooth* fibers *without varicosities* were distributed sparsely in the ventrolateral portion of the nucleus, especially in its caudal half.

In the internal capsule (Fig. 5D), fine 5-HT fibers with small varicosities,

corresponding to C-fibers, were distributed sparsely. In addition, transversely running 5-HT fibers forming loose bundles were also observed. These bundles were composed largely of C-fibers, with a few B-fibers also evident. On the basis of their shape and location, these 5-HT fiber bundles seemed to correspond to the same neural structures as the ChAT-immunostaining strips described above.

DISCUSSION

The present results allowed us to compare systematically the distribution patterns and density of cholinergic neurons and serotonergic fibers within the neostriatum, and thereby evaluate the importance of their interactions for the overall function of this key behavioral structure.

The cholinergic system of the neostriatum

The mammalian neostriatum is characterized by one of the highest concentrations of AchE in the brain (McGeer et al., 1961; Barbeau, 1962), and by its patch and matrix compartmental representation of AchE (Graybiel and Ragsdale, 1978; Graybiel et al.,1981). Butcher et al. (1975) used a pharmaco-histochemical method to show that AchE was present not only in cholinergic neurons whose cell bodies are located in the neostriatum, but also in axons whose cell bodies are located in " non-cholinergic" structures, such as the substantia nigra. Subsequently, Eng et al. (1974) and Singh and McGeer (1974) improved on the selectivity of localizing cholinergic neurons by use of ChAT-immunohistochemistry. They showed that ChAT is found only within cholinergic cell bodies and their axons. Their technique has provided the most selective method yet available to assess the distribution and morphological characteristics of cholinergic elements within a given brain structure.

Parent et al. (1980) have proposed that the cat neostriatum is structured heterogeneously in terms of the fine morphology and distribution of its AchE-containing neurons. In a subsequent study also undertaken on the cat neostriatum, Kimura et al. (1981) found large, well-stained and loosely packed ChAT cells by use of an antiserum raised in rabbit against human ChAT. Their neostriatal cholinergic cells had distinct morphological features with dense terminal fields. In addition, they had large perikarya (25-35 μm), and a few long dendrites with few spines and branches. No terminal boutons were observed on the surface of their somata. Such cells were distributed widely throughout the neostriatum.

In the Kimura et al. (1981) study, the pallidal ChAT cells were large-sized, ovoid or spindle-shaped, and they possessed few dendrites with many branches. These cells were a mixture of purely cholinergic and cholinoceptive-cholinergic types.

In relation to the patch and matrix compartments of the cat neostriatum, Graybiel et al. (1986) showed that cholinergic neuropils are preferentially distributed within the matrix, whereas both cholinergic neuropils and cholinergic perikarya are distributed within both the patch and the matrix.

More recent immunohistochemical studies have shown that the largest of the neostriatum's quite-rare intrinsic aspiny neurons are immunoreactive for ChAT, and that the smaller of them are also immunoreactive to somatostatin, neuropeptide Y, glutamate decarboxyrase or parvalbumin (Kita and Kitai, 1988; Chesselet and Graybiel, 1986; Kubota and Kawaguchi, 1993). In the present study, most of the ChAT cells in the caudate nucleus and putamen were classified as aspiny neurons (Kimura et al., 1981). In addition, we found examples of larger-sized ChAT cells in the globus pallidus. They, too, were purely cholinergic and cholinoceptive-cholinergic (Kimura et al., 1981).

Our ChAT cells were not evenly distributed in the caudate nucleus, putamen and globus pallidus (viz., Parent et al., 1980). Our results thereby supported the concept of a heterogeneous organization of the neostriatum and a species-specific distribution of cholinergic cells, as advanced previously for the neostriatum of the rat (Kubota and Kawaguchi, 1993; Schwaber et al., 1987) and non-human primate (Everitt et al., 1988; Mesulam et al., 1984).

Serotonergic innervation of the neostriatum

Among the raphe nuclei, the dorsal one is the origin of the major ascending serotonergic pathway. This nucleus is the near-exclusive (dominant) source of the raphe-striatal pathway (Azmitia and Segal, 1978; Becquet et al., 1990; Moore et al., 1978). A topographical distribution of serotoninergic terminals in the neostriatum of the rat and the caudate nucleus of the cat were first established by the combined use of microdissection techniques and biochemical assays (Ternaux et al., 1977). In both species, 5-HT terminals were localized largely in the ventrocaudal region of the tested structure. In this area of both species and structures, the 5-HT levels were among the highest values found in the brain (17 ng/mg protein). In this same study (Ternaux et al., 1977), the density of 5-HT terminals decreased progressively from the caudal to the

rostral plane of the rat neostriatum and the cat caudate nucleus. The lowest level of 5-HT was found in the dorsorostral zone of both structures. It contained ~ X4 less 5-HT than the ventrocaudal zone.

The distribution of 5-HT-containing nerve fibers in the striatum of rat, cat and non-human primate, have also been studied by use of a modified peroxidase-anti peroxidase method that employed 5-HT antiserum without pretreatment (Mori et al., 1985). In the neostriatum, the immunoreactive fibers had distinct varicosities, and they formed a fine network. For the generalized vertebrate, Sano et al. (1982) divided such 5-HT fibers into three types. Their A-fibers collateralized into B-fibers, and then very thin C-fibers (ground fibers) containing small varicosities, 0.5-1.0 μm in diameter. In the rat neostriatum, this laboratory found that the concentration of 5-HT fibers was at its highest in the ventral, medial and caudal portions of the structure. In the cat, their highest concentration of 5-HT fibers was in the medial, ventral (the fundus caudati) and caudal divisions of the caudate nucleus, and in the medial and caudal parts of the putamen (Mori et al., 1985). Our present results were essentially similar to those reported from Sano's laboratory (Sano et al., 1982; Mori et al., 1985). One exception was that our 5-HT fibers had a smaller range of values for the diameter of their varicosities (i.e., 1.0-3.0 μm in (Mori et al., 1985) vs. usually 0.5-1.0 μm, and very few > 2.0 μm in the present study). In addition, we found a much higher concentration of C-fibers in the globus pallidus than in the neostriatum.

We found no significant difference in the density and/or distribution of 5-HT fibers in the patch and matrix components of the neostriatum. Medium spiny GABA projection neurons have been shown previously to be located in both of these compartments (Penny et al., 1988; Kawaguchi et al., 1989). Their number is as many as 90-95% of the total striatal cell population. Most recently, we obtained double stains of ChAT cells and 5-HT fibers in a single section of the cat neostriatum (Okumura et al., 1999). Our preliminary results have shown a relatively small number of terminal 5-HT fibers with varicosities that are in close apposition to the proximal dendrites and somata of ChAT-containing large aspiny neurons. The far-more-profuse other 5-HT terminal endings that we identified have also innervated the GABA projection neurons.

These results suggest that 5-HT fibers terminate not only on the intrinsic ChAT cells but also on the GABA projection neurons, and that 5-HT fibers exert inhibitory (Vizi et al., 1981; Jackson et al., 1988; Mijnster et al., 1998; Yamamoto et al., 1995) and/or modulatory effects (Cassel and Jeltsch. 1995) on the activities of both intrinsic and projection neurons depending on their receptor characteristics such as 5-HT1 or 5-HT2 (Quirion and Richard, 1987; Morilak and Ciaranello, 1993; Ward and Dorsa, 1996; Cornea-Hébert et al., 1999).

Functional implication of cholinergic and serotonergic innervation

It is well established that the striatum is innervated by 5-HT neurons. The release of 5-HT from the cat caudate nucleus has been demonstrated in vivo (Boireau et al., 1976). Furthermore, 5-HT terminals have been identified at the ultramicroscopic level using a combined immunohistochemical and radioautographic technique (Soghomonian et al., 1989). As yet, however, there has been little information about the *precise topographical association* within the striatum between the distribution of 5-HT terminals and that of cholinergic cells. Such a topographic study would be timely because the 5-HT innervation of the striatum must be a fundamental aspect of extrapyramidal function. For example, on the basis of biochemical lesion studies, Chase (1974) has postulated that a critical balance between the activity of dopaminergic and 5-HT neurons is required for the elaboration of normal posture and movement. Our results suggest that the 5-HT-dominated raphe-striatal projection may contribute to the normal operation of the neostriatum by modulating the activity level of both its projection neurons and its intrinsic neurons.

REFERENCES

Azmitia EC, Segal M. 1978. An autoradiographic analysis of the differential ascending projections of the dorsal and median raphe nuclei in the rat. J Comp Neurol 179:641-667.

Barbeau A. 1962. The pathogenesis of Parkinson's disease: a new hypothesis. J Can Med Assoc 87:802-807.

Becquet D, Faudon M, Hery F. 1990. The role of serotonin release and autoreceptors in the dorsalis raphe nucleus in the control of serotonin release in the cat caudate nucleus. Neuroscience 39:639-647.

Berman A, Jones EG. 1982. The thalamus and basal telencephalon of the cat. Madison: The University of Wisconsin Press.

Boireau A, Ternaux JP, Bourgoin S, Hery F, Glowinski J, Hamon M. 1976. The determination of picogram levels of 5-HT in biological fluids. J Neurochem 26:201-204.

Bolam JP, Ingham CA, Smith AD. 1984. The section-Golgi-impregnation procedure-3. Combination of Golgi-impregnation with enzyme histochemistry and electron microscopy to characterize acetylcholinesterase-containing neurons in the rat neostriatum. Neuroscience 12:687-709.

Butcher LL, Talbot K, Bilezikjian L. 1975. Acetylcholinesterase neurons in dopamine-containing regions of the brain. J Neural Transm 37:127-153.

Cassel JC, Jeltsch H. 1995. Serotonergic modulation of cholinergic function in the central nervous system: cognitive implications. Neuroscience 69:1-41.

Chase TN. 1974. Serotonergic mechanisms and extrapyramidal function in man. Adv Neurol 5:31-39.

Chesselet MF, Graybiel AM. 1986. Striatal neurons expressing somatostatin-like immunoreactivity: evidence for a peptidergic interneuronal system in the cat. Neuroscience 17:547-571.

Cornea-Hébert V, Riad M, Wu C, Singh SK, Descarries L. 1999. Cellular and subcellular distribution of the serotonin 5-HT2A receptor in the central nervous system of adult rat. J Comp Neurol 409:187-209.

Cote S, Silva R, Cuello AC. 1993. Current protocol for light microscopy immunocytochemistry. In: Cuello AC, ed. Immunohistochemistry II. West Sussex: John Wiley & Sons Ltd:148-167.

Desban M, Gauchy C, Kemel ML, Besson MJ, Glowinski J. 1989. Three-dimensional organization of the striosomal compartment and patchy distribution of striatonigral projections in the matrix of the cat caudate nucleus. Neuroscience 29:551-566.

Eng LF, Uyeda CT, Chao LP, Wolfgram F. 1974. Antibody to bovine choline acetyltransferase and immunofluorescent localisation of the enzyme in neurones. Nature 250:243-245.

Everitt BJ, Sirkia TE, Roberts AC, Jones GH, Robbins TW. 1988. Distribution and some projections of cholinergic neurons in the brain of the common marmoset, Callithrix jacchus. J Comp Neurol 271:533-558.

Gerfen CR. 1992. The neostriatal mosaic: multiple levels of compartmental organization in the basal ganglia. Annu Rev Neurosci 15:285-320.

Gerfen CR, Herkenham M, Thibault J. 1987. The neostriatal mosaic: II. Patch- and matrix-directed mesostriatal dopaminergic and non-dopaminergic systems. J Neurosci 7:3915-3934

Grace AA, Llinas R. 1985. Morphological artifacts induced in intracellularly stained neurons by dehydration: circumvention using rapid dimethyl sulfoxide clearing. Neuroscience 16:461-475.

Graybiel AM, Baughman RW, Eckenstein F. 1986. Cholinergic neuropil of the striatum observes striosomal boundaries. Nature 323:625-627.

Graybiel AM, Ragsdale CWJ. 1978. Histochemically distinct compartments in the striatum of human, monkeys, and cat demonstrated by acetylthiocholinesterase staining. Proc Natl Acad Sci USA 75:5723-5726.

Graybiel AM, Ragsdale CW, Yoneoka ES, Elde RP. 1981. An immunohistochemical study of enkephalins and other neuropeptides in the striatum of the cat with evidence that the opiate peptides are arranged to form mosaic patterns in register with the striosomal compartments visible by acetylcholinesterase staining. Neuroscience 6:377-397.

Jackson D, Stachowiak MK, Bruno JP, Zigmond MJ. 1988. Inhibition of striatal acetylcholine release by endogenous serotonin. Brain Res 457:259-266.

Jimenez-Castellanos J, Graybiel AM. 1987. Subdivisions of the dopamine-containing A8-A9-A10 complex identified by their differential mesostriatal innervation of striosomes and extrastriosomal matrix. Neuroscience 23:223-242.

Kawaguchi Y, Wilson CJ, Emson PC. 1989. Intracellular recording of identified neostriatal patch and matrix spiny cells in a slice preparation preserving cortical inputs. J Neurophysiol 62:1052-1068.

Kekesi K, Matsuyama K, Mori S, Dobolyi A, Juhasz G. 1997. Extracellular monoamine and amino acid levels in the caudate nucleus, thalamic nuclei(VA/VL) and pontine reticular formation in the freely moving cat. Neurosci Res 21(suppl):S182.

Kemp JM, Powell TP. 1971. The structure of the caudate nucleus of the cat: light and electron microscopy. Philos Trans R Soc Lond B Biol Sci 262:383-401.

Kimura H, McGeer PL, Peng JH, McGeer EG. 1981. The central cholinergic system studied by choline acetyltransferase immunohistochemistry in the cat. J Comp Neurol 200:151-201.

Kita H, Kitai ST. 1988. Glutamate decarboxylase immunoreactive neurons in rat neostriatum: their morphological types and populations. Brain Res 447:346-352.

Kobayashi Y, Matsuyama K, Mori S. 1994. Distribution of serotonin cells projecting to the pontomedullary reticular formation in the cat. Neurosci Res 20:43-55.

Kubota Y, Kawaguchi Y. 1993. Spatial distributions of chemically identified intrinsic neurons in relation to patch and matrix compartments of rat neostriatum. J Comp Neurol 332:499-513.

McGeer PL, Boulding JE, Gobson WC, Foulkes RG. 1961. Drug-induced extrapyramidal reactions. J Am Med Assoc 177:665-670.

Mesulam MM, Mufson EJ, Levey AI, Wainer BH. 1984. Atlas of cholinergic neurons in the forebrain and upper brainstem of the macaque based on monoclonal choline acetyltransferase immunohistochemistry and acetylcholinesterase histochemistry. Neuroscience 12:669-686.

Mijnster MJ, Galis-de Graaf Y, Voorn P. 1998. Serotonergic regulation of neuropeptide

and glutamic acid decarboxylase mRNA levels in the rat striatum and globus pallidus: studies with fluoxetine and DOI. Brain Res Mol Brain Res 54:64-73.

Moore RY, Halaris AE, Jones BE. 1978. Serotonin neurons of the midbrain raphe: ascending projections. J Comp Neurol 180:417-438.

Mori S, Ueda S, Yamada H, Takino T, Sano Y. 1985. Immunohistochemical demonstration of serotonin nerve fibers in the corpus striatum of the rat, cat and monkey. Anat Embryol (Berl) 173:1-5.

Morilak DA, Ciaranello RD. 1993. 5-HT2 receptor immunoreactivity on cholinergic neurons of the pontomesencephalic tegmentum shown by double immunofluorescence. Brain Res 627:49-54.

Okumura T, Dobolyi A, Matsuyama K, Kakigi R, Mori S. 1999. Cholinergic and serotonergic interactions in the caudate nucleus in relation to behavioral control in cats. Soc Neurosci Abstr 25:1155.

Okumura T, Matsuyama K, Mori S. 1998. Effect of carbachol perfusion of the caudate nucleus on extracellular monoamine levels in the brain of freely moving cats. Jpn J Physiol 48(suppl):S154.

Parent A, O'Reilly-Fromentin J, Boucher R. 1980. Acetylcholinesterase-containing neurons in cat neostriatum: a morphological and quantitative analysis. Neurosci Lett 20:271-276.

Penny GR, Wilson CJ, Kitai ST. 1988. Relationship of the axonal and dendritic geometry of spiny projection neurons to the compartmental organization of the neostriatum. J Comp Neurol 269:275-289.

Phelps P, Houser C, Vaughn J. 1985. Immunocytochemical localization of choline acetyltransferase within the rat neostriatum: a correlated light and electron microscopic study of cholinergic neurons and synapses. J Comp Neurol 238:286-307.

Quirion R, Richard J. 1987. Differential effects of selective lesions of cholinergic and dopaminergic neurons on serotonin-type 1 receptors in rat brain. Synapse 1:124-130.

Sano Y, Takeuchi Y, Kimura H, Goto M, Kawata M, Kojima M, Matsuura T, Ueda S,

Yamada H. 1982. Immunohistochemical studies on the processes of serotonin neurons and their ramification in the central nervous system-with regard to the possibility of the existence of Golgi's rete nervosa diffusa. Arch Histol Jpn 45:305-316.

Schwaber JS, Rogers WT, Satoh K, Fibiger HC. 1987. Distribution and organization of cholinergic neurons in the rat forebrain demonstrated by computer-aided data acquisition and three-dimensional reconstruction. J Comp Neurol 263:309-325.

Singh VK, McGeer PL. 1974. Cross-immunity of antibodies to human choline acetyltransferase in various vertebrate species. Brain Res 82:356-359.

Soghomonian JJ, Descarries L, Watkins KC. 1989. Serotonin innervation in adult rat neostriatum. II. Ultrastructural features: a radioautographic and immunocytochemical study. Brain Res 481:67-86.

Steinbusch HW, Nieuwenhuys R, Verhofstad AA, Van der Kooy D. 1981. The nucleus raphe dorsalis of the rat and its projection upon the caudatoputamen. A combined cytoarchitectonic, immunohistochemical and retrograde transport study. J Physiol Paris 77:157-174.

Steinbusch HW, Verhofstad AA, Joosten HW. 1978. Localization of serotonin in the central nervous system by immunohistochemistry: description of a specific and sensitive technique and some applications. Neuroscience 3:811-819.

Takeuchi Y, Kimura H, Sano Y. 1982. Immunohistochemical demonstration of the distribution of serotonin neurons in the brainstem of the rat and cat. Cell Tissue Res 224:247-267.

Tanaka H, Mori S, Kimura H. 1992. Developmental changes in the serotoninergic innervation of hindlimb extensor motoneurons in neonatal rats. Dev Brain Res 65:1-12.

Ternaux JP, Hery F, Bourgoin S, Adrien J, Glowinski J, Hamon M. 1977. The topographical distribution of serotoninergic terminals in the neostriatum of the rat and the caudate nucleus of the cat. Brain Res 121:311-326.

Vizi ES, Hársing LGJ, Zsilla G. 1981. Evidence of the modulatory role of serotonin in acetylcholine release from striatal interneurons. Brain Res 212:89-99.

Ward RP, Dorsa DM. 1996. Colocalization of serotonin receptor subtypes 5-HT2A, 5-HT2C, and 5-HT6 with neuropeptides in rat striatum. J Comp Neurol 370:405-414.

Wilson CJ, Groves PM. 1980. Fine structure and synaptic connections of the common spiny neuron of the rat neostriatum: a study employing intracellular inject of horseradish peroxidase. J Comp Neurol 194:599-615.

Yamamoto BK, Nash JF, Gudelsky GA. 1995. Modulation of methylenedioxymethamphetamine-induced striatal dopamine release by the interaction between serotonin and gamma-aminobutyric acid in the substantia nigra. J Pharmacol Exp Ther 273:1063- 1070.

FIGURE LEGENDS

Figure 1. Distribution of ChAT-immunopositive cells in the cat neostriatum and its surrounding areas. Each panel shows the drawing of part of a separate transverse section (Horsley-Clarke co-ordinates, A19.3-12.7) taken from a single cat. Each dot represents the location of one neuron labeled specifically for ChAT. Arrows at A15.5-12.7 indicate ChAT-immunostained strips in the internal capsule. Abbreviations: AC, nucleus accumbens; CA, caudate nucleus; GP, globus pallidus; IC, internal capsule; PU, putamen; SI, substantia innominata. Scale bar at A16.4 = 1mm for all drawings.

Figure 2. Transverse plane photomicrographs of ChAT-immunopositive cells in the cat neostriatum. Shown are representative levels of the caudate nucleus (A, D), putamen (B), globus pallidus (E) and internal capsule (C, F). ChAT cells indicated by arrows in the higher-magnification photomicrographs (D-F) correspond to labeled cells indicated by arrows in the lower-magnification A-C photomicrographs. Black arrows are for multipolar-shaped cells, and white arrows are for pyramidal-shaped cells. Thin arrow in E indicates a ChAT-positive terminal bouton-like structure closely apposed to a ChAT cell. Abbreviations as in Fig. 1. Scale bar in F = 100 μm for A-C, and 25 μm for D-F.

Figure 3. Low-magnification photographs of ChAT-immunostained transverse-plane sections of the cat neostriatum. Shown are levels A18.3, 16.4 and 14.5 in a single cat. Areas indicated by asterisks (*) are weakly stained zones surrounded by more darkly stained areas. These weakly vs. darkly stained areas may correspond to the "patch" vs. "matrix" organization reported by Graybiel et al. (8). Abbreviations as in Fig. 1. Scale bar in A18.3 = 1mm for all photographs.

Figure 4. Distribution of 5-HT-immunopositive fibers in the cat neostriatum and its surrounding areas A: Low magnification photographs of 5-HT-immunostained

transverse sections of the neostriatum at levels A18.3, 16.4 and 14.5 in a single cat. At each level, the section shown was adjacent to the section shown in Fig. 3. B: Dorsoventral distribution pattern of 5-HT-immunopositive fibers in the caudate nucleus at A16.4. The camera lucida a-c drawings correspond to areas indicated by the a-c squares at level A16.4 in A. C: Distribution pattern of 5-HT-immunopositive fibers in the putamen at levels A18.3, 16.4 and 14.5. Same drawing/square arrangement as in B. For B-C, each line and dot represents a single 5-HT fiber, and thin lines indicate relatively large blood vessels. Abbreviations as in Fig. 1. Scale bar in A18.3 in A = 1 mm for all photomicrographs, and that in B-a = 300 μm for all drawings in B and C.

Figure 5. Pairs of low- and high-gain photomicrographs of 5-HT-immunopositive fibers in the cat neostriatum. Shown are representative levels of the dorsal (A) and ventral (B) caudate nucleus, putamen (C), and internal capsule (D). For each pair, the right-side one is a higher-magnification photomicrograph taken from the area indicated by a square in the left-side, lower-magnification figure. All photomicrographs were taken from the same section as shown in Figure 4A (A16.4). Thin arrows indicate B-fibers, as defined by Sano et al. (3), and a thick arrow indicates a particularly thick fiber with few varicosities. Abbreviations as in Fig. 1. Scale bar in D on the right side = 100 μm for all photomicrographs on the left side, and 25 μm for all photomicrographs on the right side.

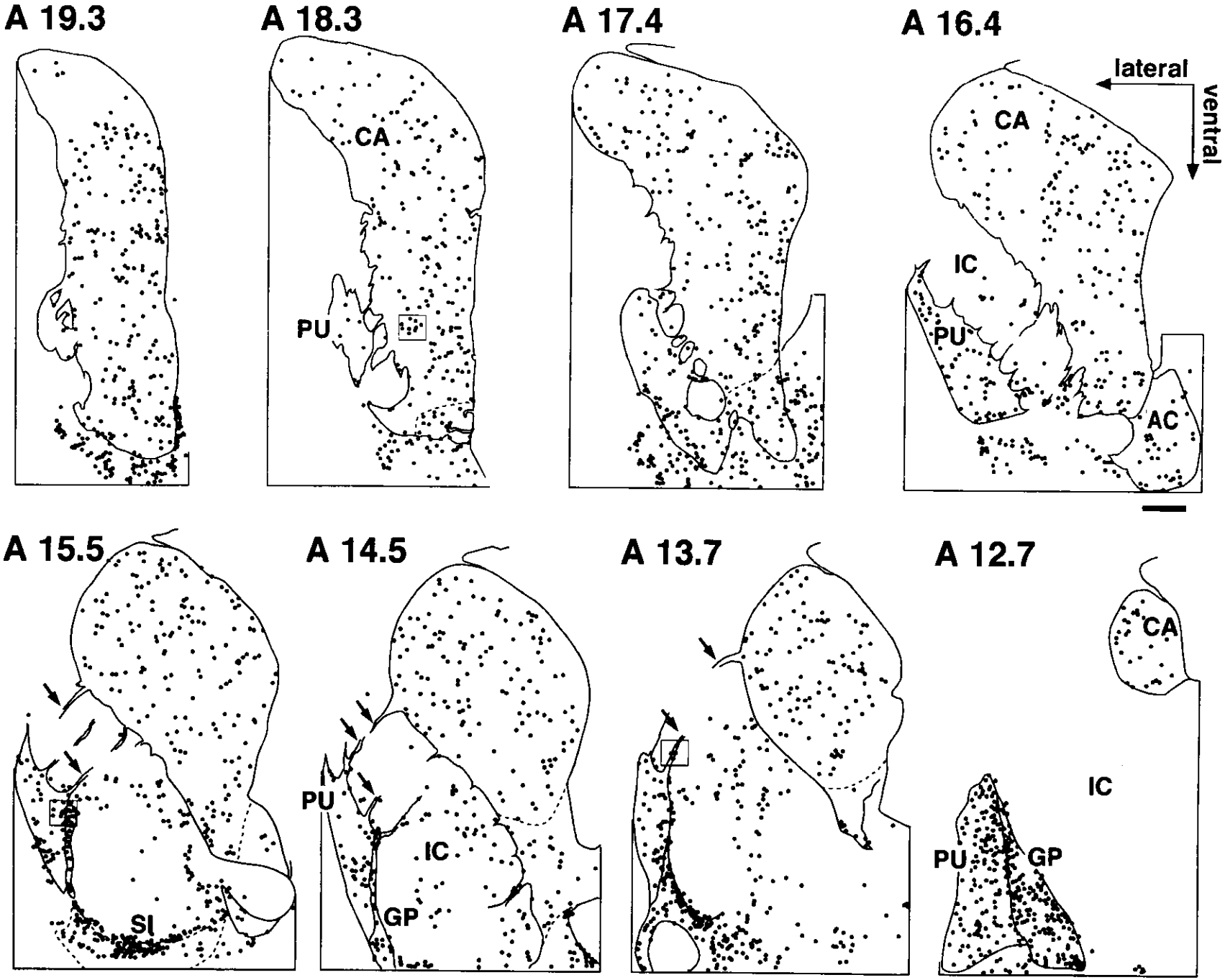
A 19.3
A 18.3
CA
PU
A 17.4
A 16.4
lateral
ventral
CA
IC
PU
AC
A 15.5
SI
A 14.5
PU
IC
GP
A 13.7
A 12.7
CA
IC
PU
GP

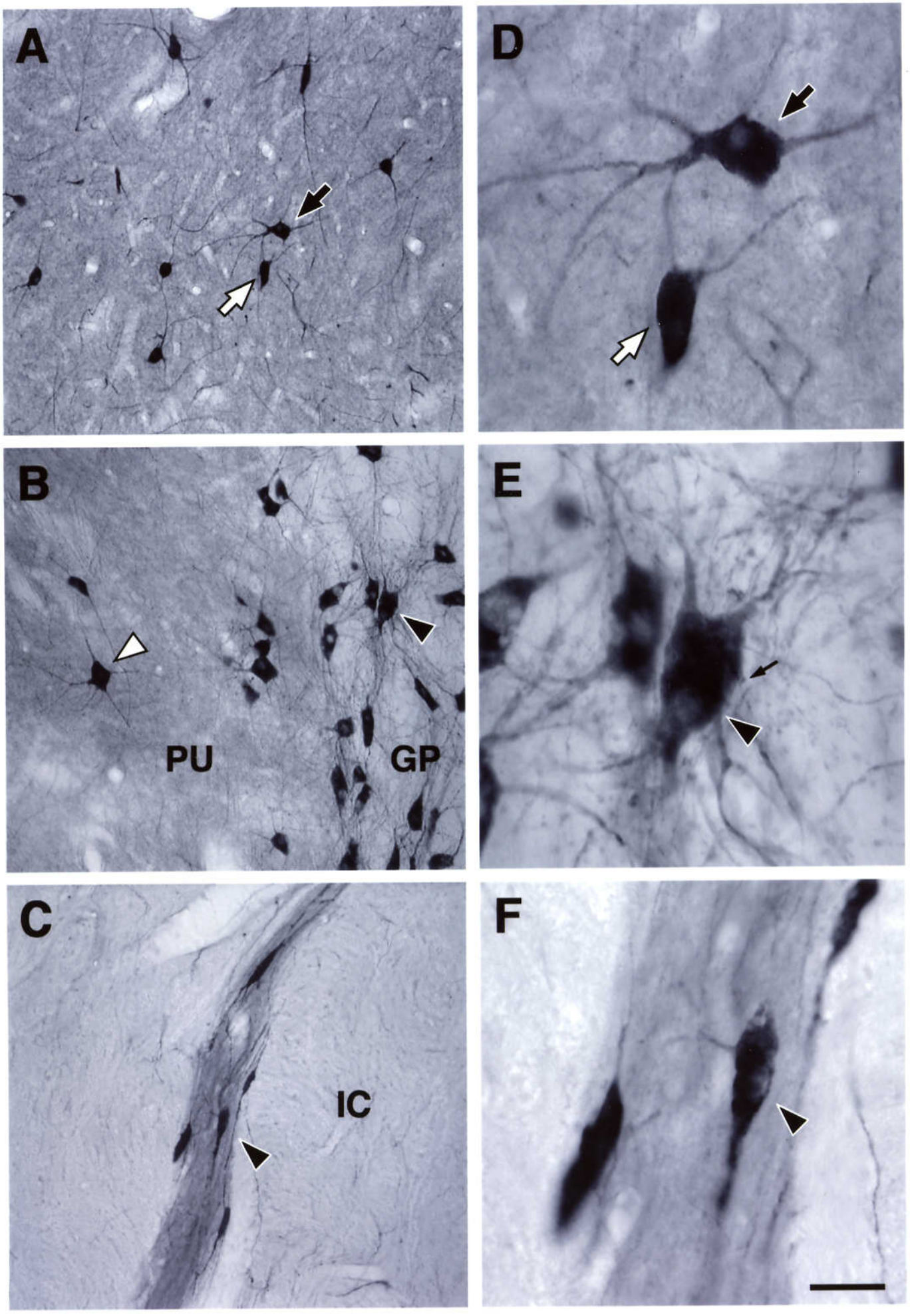
A
D
B
PU
GP
E
C
IC
F

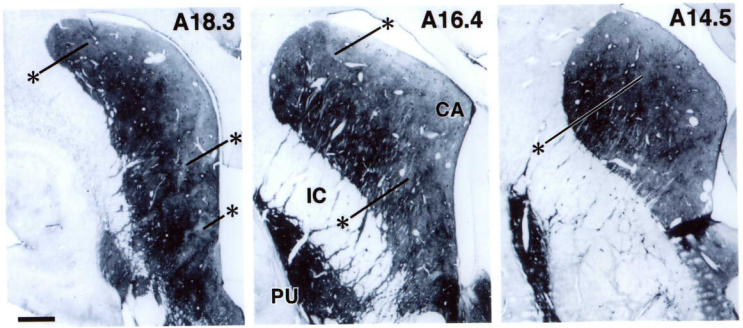
A18.3
A16.4
CA
IC
PU
A14.5

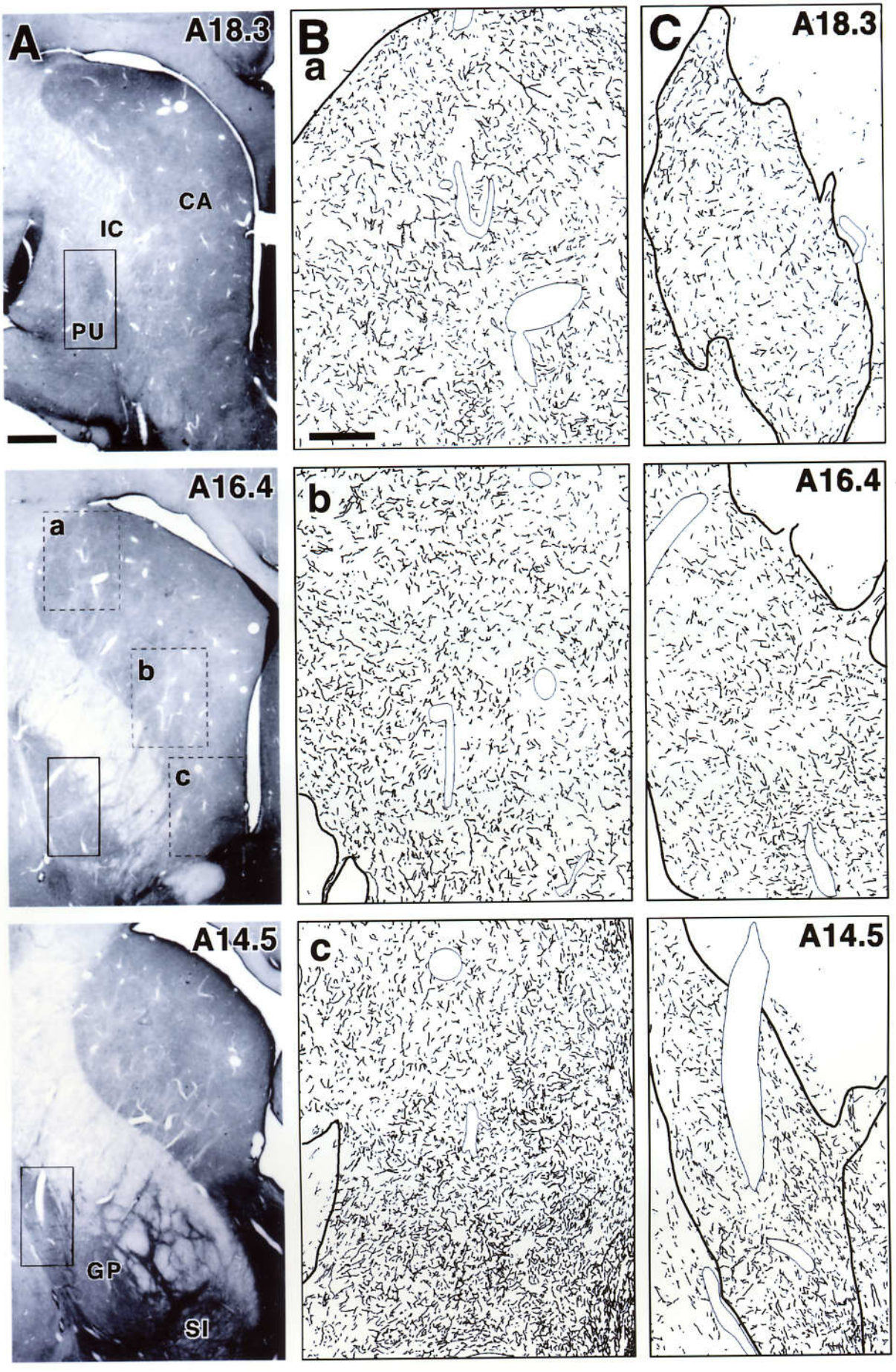
A
A18.3
CA
IC
PU
B
a
C
A18.3
A16.4
a
b
c
b
A16.4
A14.5
GP
SI
c
A14.5

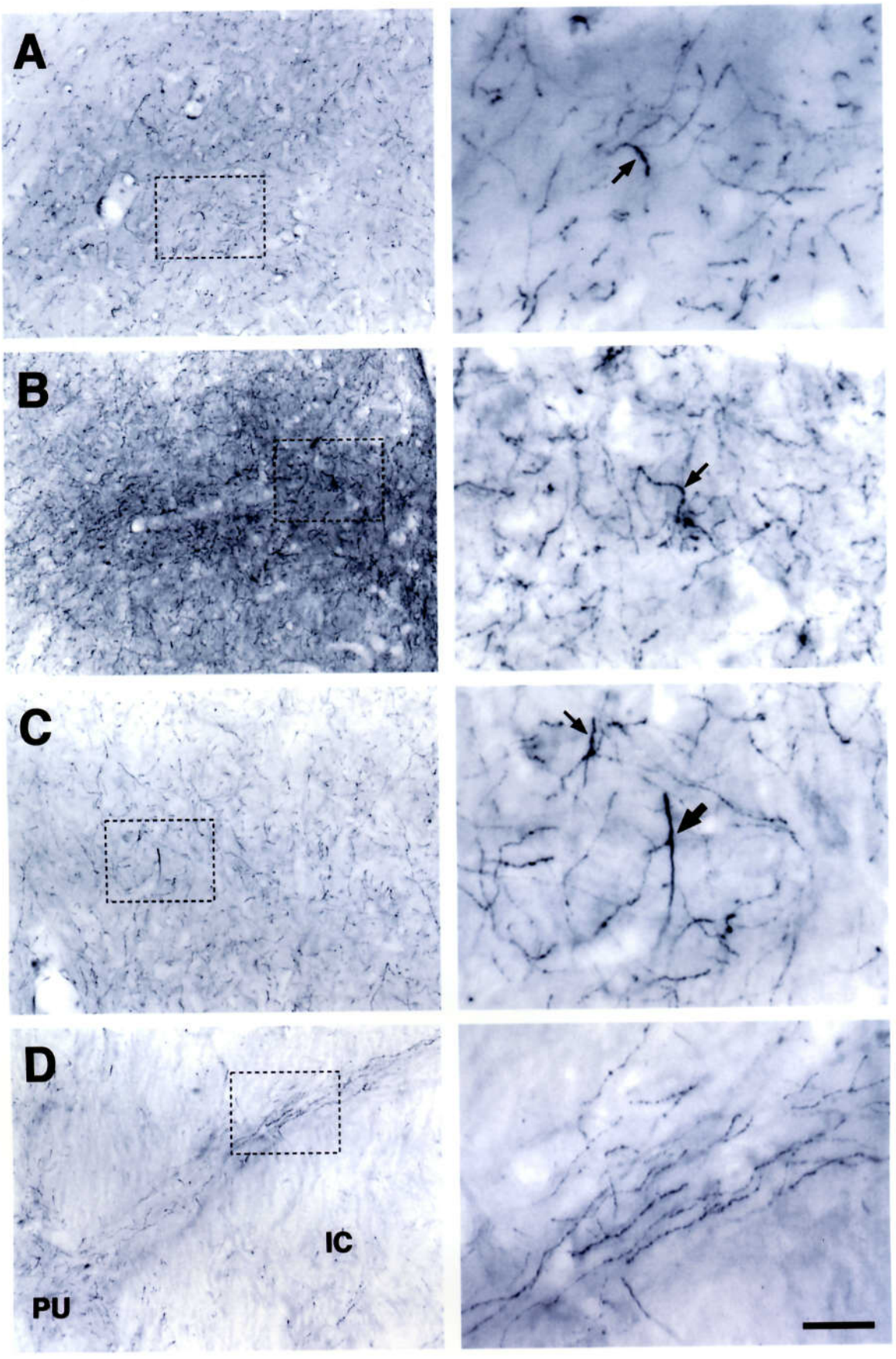
A
B
C
D
IC
PU

Part 2

Distribution and fine morphology of neostriatal output neurons, and serotonergic innervation to the output neurons and cholinergic interneurons in the cat

Tetsu OKUMURA

Doctor of Philosophy

Department of Physiological Sciences,

School of Life Sciences,

The Graduate University for Advanced Studies

and

Department of Biological Control System,

National Institute for Physiological Sciences,

Myodaiji, Okazaki, 444-8585

JAPAN

Number of text pages: 36 (including a title page)

Number of figures: 10

ABSTRACT

To characterize the distribution and fine morphology of neostriatal output neurons, retrograde neural tracer, biotinylated dextran amine (BDA) was focally injected into three major target nuclei of the striatum: the globus pallidus (GP), entopeduncular nucleus (EP) and substantia nigra pars reticulata (SNR). We found a general tendency that GP- and EP-projection cells to occur at highest density in the dorsal part of the caudate body and caudate head, respectively, whereas SNR-projection cells had their highest density in a more ventral portion of the head and body of the caudate nucleus. At those rostro-caudal levels where the density of GP-, EP- and SNR-projection cells were highest, the density of BDA retrogradely labeled cells in the putamen tended to be the highest. The majority of the labeled output projection neurons in the caudate nucleus were small to medium sized and multipolar in shape. The range of their soma diameters was 12-27 μm (long axis) X 6-17 μm (short axis). They had 4–8 primary (1^{st}-order) dendrites. A number of spines on the remote dendrites were also BDA-labeled. At the primary dendrites and the initial part of the secondary dendrites, spines tended to be absent. There was no significant morphological difference in the characteristics and the size of the retrogradely labeled output cells with BDA injections into the GP, EP and SNR. 5-HT- and ChAT-immunohistochemistry were also applied for the neostriatal sections to investigate 5-HT innervation to BDA-labeled output neurons and ChAT positive interneurons. ChAT positive cells were large-sized and aspiny. Somata and dendrites of output neurons projecting to the GP, EP and SNR and those of ChAT positive interneurons were densely surrounded by thin 5-HT fibers (C-fibers) and varicosities. In addition, the spines of striatal output neurons were closely apposed by a number of fine 5-HT varicosities.

INTRODUCTION

The vertebrate striatum is innervated by serotonin (5-HT) containing neurons in the dorsal raphe (Steinbusch et al., 1978; Steinbusch et al., 1981). 5-HT containing nerve fibers in the striatum of the rat, cat and non-human primate had distinct varicosities that were collateralized into a fine network. Sano et al. (1982) divided such 5-HT fibers into A, B and C types. The stem fibers, which originated from cell bodies, branched into either A-fibers (tract fibers) with varicosities of 4-5 μm in diameter or B-fibers (branching fibers) with varicosities of 2-3 μm in diameter. These thick A- and B-fibers further branched off to form very thin C-fibers (ground fibers). These C-fibers contained a great number of small varicosities, 0.5-1.0 μm in diameter. In the cat neostriatum, the majority of 5-HT fibers were C-fibers forming dense and fine networks (Okumura et al., in press). We found highest concentration of 5-HT fibers in the medial, ventral (the fundus caudati) and caudal divisions of the caudate nucleus, and in the medial and caudal parts of the putamen and the entire globus pallidus. In the caudate nucleus, no significant difference was found in the density and/or distribution of 5-HT fibers in the patch and matrix compartments, where medium spiny GABAergic (GABA, γ-aminobutylic acid) neurons are located.

GABA neurons, which are as many as 80-90% of the total striatal cells, have been identified as output projection neurons, while remaining large-sized aspiny neurons which contain Ach as intrinsic neurons or interneurons (Kita et al., 1988; Gerfen, 1992). In considering relatively rich distribution of 5-HT fibers in the striatum, it will be interesting to elucidate the precise topographical association within the striatum between the distributions of terminal 5-HT fibers and those of GABAergic output neurons and cholinergic interneurons. Our preliminary study has already shown a number of terminal 5-HT fibers with varicosities that are in close apposition to the proximal dendrites and somata of choline acetyltransferase (ChAT)-

containing interneurons (Okumura et al., 1999a,b). In studying and understanding functinal implication of serotonergic innervation to GABA output neurons, it seems important to identify the remote projection sites of output neurons. With regard to the remote projection sites of output neurons, little information is available excepting the finding that outputs to the globus pallidus (GP), entopeduncular nucleus (EP) and substantia nigra pars reticulata (SN) appeared to come from different population of striatal neurons (Beckstead and Cruz, 1986).

Among inputs to the striatum, the role played by nigrostriatal dopamine system has been extensively studied in relation to the movement disorders and hyperactivity (Albin et al., 1989; Carey et al., 1998; Russell et al., 1998). It appears that dopamine receptors reside on the Ach-containing interneurons, thus nigrostriatal system exerting a direct, tonic inhibitory effect on some or all of the cholinergic cells in the caudate nucleus (Chase, 1974). It is also generally assumed that GABA serves as an inhibitory neurotransmitter for small interneurons within the caudate nucleus as well as for striatal efferents to GP and SN (Alexander and Crutcher, 1990). With regard to the function of the 5-HT system, Chase (1974) suggested that dopamine and 5-HT containing neuronal system ordinarily operate in a balanced arrangement, and that diminished dopamine-mediated function may evoke a secondary reduction in the activity of serotonergic neurons. Recently Gainetdinov et al. (1999) tried to determine whether serotonergic chemical agent affects motor activity through modulation of striatal dopamine (DA) release. They demonstrated that serotonergic neurotransmission can modulate hyperactivity without producing concurrent changes in extracellular striatal DA concentrations.

In this study, therefore, we first attempted to identify the distributions of output neurons in the caudate nucleus, which project selectively to the GP, EP and SNR. These output neurons were retrogradely identified by focally injecting biotinylated dextran amine (BDA) into each of the target nuclei. With double stains

of BDA-labeled cells and 5-HT fibers in a single section of the cat neostriatum, we then studied the topographical association between the distributions of output cells projecting to the GP, EP and SNR and those of terminal 5-HT fibers. With double stains of ChAT cells and 5-HT fibers in the neighboring striatal sections, we also studied the topographical association between the distributions of ChAT cells in the regions containing output neurons and those of terminal 5-HT fibers. A number of terminal fibers were found to intertwine both the somata and distal dendrites of output neurons, irrespective of their remote projections sites, and interneurons with some of the varicosities in close apposition to them. Preliminary results have been published in abstracts (Okumura et al., 1999a,b).

MATERIALS AND METHODS

In the present study, two groups of cats (total 8 animals) were used in order to investigate (1) the distribution and fine morphology of the neostriatal output neurons and the serotonergic innervation to them (n=6), and (2) the serotonergic innervation to the cholinergic interneurons in the neostriatum (n=2).

Labeling of the neostriatal output cells and 5-HT fibers

BDA injection Experiments were performed on six young adult cats (two female and four male) weighing 2.0-2.7 kg. The animals were anesthetized with sodium pentobarbital (30 mg/kg, I.P.; supplementary doses, 5 mg/kg, I.V.). Prior to anesthesia, atropine (40 μg/kg) was injected subcutaneously to suppress excessive salivation and secretions of the respiratory tract. The head was shaved, and then the cat was fixed in a stereotaxic apparatus by using atraumatic ear bars. A small craniotomy was made in the right side of the calvarium to expose the cerebral surface. In each cat, Hamilton microsyringe fitted with a 25-guage needle was inserted stereotaxically through the craniotomy either into the GP (Horseley-Clark coordinates: A11.5, R6.5, H-1.35; n=2), the EP (A5.1, R4.4, H-3.4; n=2) or the SNR (A13.2, R8.2, H+0.5; n=2) via the cerebral cortex. The microsyringe was filled with 20 % biotinylated dextran amine (BDA, 3000 MW, Molecular Probes Inc, Eugene, Oregon) solution dissolved in saline. In each nucleus, three (n=3) or six (n=3) aliquots of 50 nl BDA solution were injected through the microsyringe at 5-minute interval (total injection volume 0.15 or 0.3 μl). The syringe was left in place for an additional 15 minutes (i.e., to obviate back-fill).

After withdrawal of the syringe, the surface of the cerebral cortex was covered with a hemostatic sponge, and the craniotomy was filled with dental cement. Next, the animal was placed in an incubator, and its vital signs were monitored during recovery from anesthesia. Antibiotics were administered intramuscularly for at least

5 days after surgery. During their recovery, no abnormal behavior was observed in any of the animals. All experimental and surgical procedures were in conformity with the policies of the National Institute for Physiological Sciences, and the procedures were approved by the institute's Committee on Animal Experimentation.

Staining for BDA. Following survival periods of 7 days, the cats were deeply anesthetized with pentobarbital (40 mg/kg, I.P.) and perfused transcardially, first for 20-30 minutes with 0.01 M phosphate-buffered saline (PBS, pH 7.4, 1 liter/kg) to wash out the blood, and, subsequently, for 20-30 minutes with a fixative containing 4% paraformaldehyde, 0.1% glutaraldehyde and 0.2% picric acid in 0.1M phosphate buffer (pH 7.4, 1 liter/kg). After the perfusion procedure, the brain tissue was immediately removed and post-fixed for 1 day at 4° C in a fixative containing 4% paraformaldehyde and 0.2% picric acid in 0.1 M phosphate buffer. The tissue was then immersed for at least 5 days at 4 °C in 0.1 M phosphate buffer containing 20 % sucrose. The forebrain, including the BDA injection sites and the caudate nucleus, was cut into serial transverse sections on a cryotome at a thickness of 50 μm.

Every 5th serial section was used for determination of the distribution and morphology of retrogradely transported-BDA containing output cells in the neostriatum. These sections, in a free-floating state, were incubated overnight at room temperature in 0.1M PBS consisting of avidin-biotinylated peroxidase complex (ABC-Elite; Vector Lab, Burlingame, California) and 0.3 % Triton-X. Then, the sections were reacted with 0.01% 3,3'-diaminobendizine (DAB), 1% nickel ammonium sulfate and 0.0003% H_2O_2 in 0.05M Tris-HCl buffer for at least 20 min (Takeuchi et al., 1982). After staining, the sections were mounted on gelatin-coated glass slides, dehydrated, and coverslipped for observation. Some sections were lightly counterstained with 1% neutral red.

Double staining for BDA and 5-HT immunoreactivity. For determination of patterns of serotonergic (5-HT) innervation to output cells in the neostriatum, we used every 5th serial section immediately adjacent to those used for BDA staining. For visualizing BDA containing output cells, these sections, also in a free-floating state, were incubated overnight at room temperature in 0.1M PBS containing ABC and 0.3% Triton-X. Then, the sections were reacted with 0.01% DAB and 0.0003% H_2O_2 in 0.05M Tris-HCl buffer for at least 20 min, and BDA-containing cells were visualized as brown. After a rinse with PBS, these sections were reacted with 0.3 % H_2O_2 in 0.05M Tris-HCl buffer for at least 20 min to eliminate the remaining peroxidase activity. After several rinses with PBS, they were incubated for 2 days at room temperature with rabbit 5-HT antiserum (diluted 1:20,000) in 0.1M PBS containing 0.3% Triton-X, followed by incubations with: first, biotinylated goat anti-rabbit IgG for 2 hr; and second, ABC for 1 hr. Finally, the sections were reacted with 0.01% DAB, 1% nickel ammonium sulfate and 0.0003% H_2O_2 in 0.05M Tris-HCl buffer for at least 20 min, and 5-HT-immunopositive fibers were visualized as blue-black. After double staining, the sections were mounted onto gelatin-coated glass slides, dehydrated and cover-slipped.

Labeling of cholinergic interneurons and 5-HT fibers

Experiments were performed on two young adult male cats weighing 2.2 and 3.2 kg. They were deeply anesthetized with pentobarbital (40 mg/kg, I.P.) and perfused transcardially in the same procedure as described above. After the perfusion, the fixed brain tissue was removed immediately and post-fixed for 2 days at 4 °C in a fixative containing 4 % paraformaldehyde and 0.2 % picric acid in 0.1 M phosphate buffer. The tissue was then immersed in 0.1 M phosphate buffer

containing 20 % sucrose for at least another 2 days at 4 °C. Transverse serial sections of the forebrain were cut on a cryotome at a thickness of 50 μm.

For determination of patterns of 5-HT innervation to ChAT-containing cells (cholinergic interneurons) in the neostriatum, we used every 5th serial section of the forebrain including the neostriatum. These sections, in a free-floating state, were incubated for 2 days at 4 °C with monoclonal ChAT antibody from rat/mouse hybrid cells (diluted to 0.33 μg antibody/ml; Boehringer Mannheim Bio, Germany) in 0.1M PBS containing 0.3% Triton-X at room temperature, and then incubated: first, with biotinylated-rabbit anti-rat IgG for 1hr; and second, with ABC for 1 hr. Finally, the sections were incubated with 0.06% DAB and 0.01% H_2O_2 in 0.01M Tris-HCl buffer for 5-15 min (Cote et al., 1993), and ChAT-immunopositive cells were visualized as brown. After a rinse with PBS, the sections were reacted with 0.3 % H_2O_2 in 0.05M Tris-HCl buffer for at least 20 min. After several rinses with PBS, they were reacted according to 5-HT immunohistochemical procedure as same as that described above, and 5-HT-immunopositive fibers were visualized as blue-black. After double staining, the sections were mounted onto gelatin-coated glass slides, dehydrated and cover-slipped.

Analyses

All stained sections were examined under a light microscope equipped with a light-field condenser. We studied the locations of BDA-labeled cells in the neostriatum of single sections at levels A19.4-10.4 with an interval of 1.5 mm, and they were plotted on representative frontal planes using a software-controlled, microscopy system (Neurolucida system, MicroBrightField Inc, Colchester, Vermont). For each section, the numbers of the labeled cells in the caudate nucleus and putamen were also counted. 5-HT fibers located in the caudate nucleus of representative

sections were plotted using a camera lucida with a X20 dry objective (final magnification X200). In addition, to analyze the detailed innervation pattern of 5-HT fibers to BDA-labeled output cells and ChAT-positive cells, camera lucida drawings of their fine architecture were made with a X100 oil-immersion objective (final magnification X1000). The size and diameter of BDA-labeled cells, ChAT-positive cells and 5-HT fibers were measured at high power (X1000) under a X100 oil-immersion objective. In these measurements, no correction was made for possible shrinkage of cells and fibers as a result of the histological procedures (Grace and Llinas, 1985).

Photomicrographs were taken with a Polaroid digital microscope camera (resolution: 1600 x 1200 pixels) connected to the microscope with X1-X100 objectives. To make photomontages, the luminosity of the raw photomicrographs was modified by use of graphics software (Adobe Photoshop 5.0J) on a PC computer. The illustration plates were printed with a digital color printer (Pictrography 4000, Fujifilm Co, Japan).

Anatomical nomenclature conforms to the description of Berman and Jones (1982).

RESULTS

In the present study, we have aimed to characterize the distribution and fine morphology of neostriatal output cells projecting to three major target nuclei (GP, EP and SNR), together with the serotonergic innervation to them and cholinergic interneurons in the cat neostriatum. These aims were achieved by exactly identifying the output cells, interneurons and 5-HT fibers utilizing BDA-retrograde tracing technique, ChAT- and 5-HT-immunohistochemistry, respectively.

Distribution of the neostriatal output cells projecting to the GP, EP and SNR and their morphology

In all cats with BDA injections into the GP, EP and SNR, a large number of output cells were retrogradely labeled throughout the full rostral to caudal extent of the neostriatum (i.e., Horsley-Clarke co-ordinate, A20.0-11.5). The majority of labeled cells were multipolar and the remaining cells were fusiform or pyramidal.

1. BDA injection areas

The photomicrographs in Figure 1A-C show the center regions of BDA injection areas in three cats kept 7 days after 0.3 μl BDA injections into the GP, EP and SNR, respectively. The longest extent of BDA diffusion in the mediolateral, dorsoventral and rostrocaudal directions were 1.5, 2.0 and 1.5 mm, 1.3, 2.0 and 1.4 mm, and 1.8, 2.0 and 1.8 mm in the GP, EP and SNR, respectively. As shown in the lower drawing in A, BDA diffusion area was localized within the GP. In the other cases shown in the drawings B-C, the major injection areas were located in the EP and SNR, respectively, although their diffusion areas outspread to the optic tract (B) and the central tegmental field (FTC, C). In addition, a small BDA diffusion was observed along the track of a microsyringe through the internal capsule (B) and FTC (C).

In other three cats with 0.15 μl BDA injection, the extent of diffusion was less than those of the three cats shown in Figure 1 (not illustrated).

2. Preferential distribution of the output cells projecting to the GP, EP and SNR

In the caudate nucleus. Three photomicrographs A, B and C in Figure 2 show representative transverse planes of the caudate nucleus with BDA injections into the GP (A), EP (B) and SNR (C), respectively. As shown in these photomicrographs, BDA-labeled cells appeared as dark stained particles. Dense aggregation areas of the labeled cells were commonly observed in all cats, although there were differences in the density of cells between these animals. The zones where labeled cells were sparsely distributed (see asterisks) were also observed within the aggregation areas. These dense vs. sparse distribution areas may correspond to the "patch" vs. "matrix" organization reported by Graybiel and Ragsdale (1978).

Figure 3A-C show the overall distribution of the labeled cells in the caudate nucleus and putamen, irrespective of their size and shape, on 6 transverse planes at levels A19.4-12.9 in the cats with the injection into the GP, EP and SNR, respectively. The BDA injection into the GP resulted in the labeling of considerable numbers of output cells in the caudate nucleus and putamen (Fig. 3A). In the caudate nucleus, a total of 3859 labeled cells were distributed on the 6 planes from A19.4 to A10.9. About 96 % of the cells were located in the middle portion of the nucleus at A16.4-13.4 (the highest number, 1663 at A14.9). In this portion, labeled cells were highly concentrated in the dorsal half region. At the rostral portion (A19.4-17.9), a small number of labeled cells were sparsely distributed only in the dorsal half of the caudate nucleus. In the cat with BDA injection into the EP, a total of 1317 cells were distributed on the 6 planes from A19.4 to A13.4 (Fig. 3B). About 90 % of the cells were located in the rostral (A17.9) to middle (14.9) portions of the nucleus (the highest number, 559 at A16.4). At A19.4-16.4, most of labeled cells were highly localized in the dorsal half, but at more caudal level A14.9-13.4, they were evenly

distributed in the dorsal to ventral regions. BDA injection into the SNR also resulted in the retrograde labeling of output cells. A total of 1994 cells were distributed on the 6 planes at A19.4-10.0 (Fig. 3C). About 86 % of cells were distributed in the middle portion of the nucleus at A16.4-13.4 (the highest number, 701 at A14.9). At the rostral portion (A19.4-17.9), most cells were distributed mainly in the dorsal half of the caudate nucleus

In the putamen. In all three cats, characteristic distribution pattern of the labeled cells was also observed in the putamen, although the number of labeled cells was much smaller than that in the caudate nucleus.

In the cat with GP injection, a total of 190 cells were distributed on 6 transverse planes from A16.4 to A10.9. About 77 % of the cells were localized in the middle portion (A14.9-13.4), mainly in the dorsal half. In the cat with EP injection, a total of 260 cells were labeled at A19.4-12.4, and about 84 % of the cells were located in the rostral portion of the nucleus (A17.9-14.9). In this portion, the cells were evenly distributed in the dorsal to ventral regions. In the cat with SNR injection, a total of 438 cells were labeled at levels A19.4-10.4. About 90 % of the cells were highly localized in the rostral to middle portions at A16.4-13.4, similar to the levels at which the dense distribution was observed in the caudate nucleus. At these levels, the cells were evenly distributed in the dorsal to ventral regions.

As shown in above, the distribution pattern of BDA-labeled cells in the neostriatum were clearly different between the animals with the injection into the GP, EP and SNR. Such different distribution patterns were also found in the three cats with 0.15 μl BDA injections to the GP, EP and SNR. Figure 4A-C show the distribution of labeled cells in the neostriatum observed on the 3 representative planes, respectively. On the planes at levels A14.5 (A), A16.4 (B) and A14.0 (C), the largest numbers of the labeled cells were found to distribute. The levels in Figure 4A-C corresponded to those where labeled cells were densely distributed in the other cats

with 0.3 μl injection into GP (A14.9), EP (A16.4) and SNR (A14.9) shown in Figure 3A-C, respectively. Similar to the cats in Figure 3A-C, the labeled cells were highly localized in the dorsal half region in Figure 4A-B, and in the center region in C, respectively. These results indicate that the distribution of the output cells in the neostriatum is organized in a specific manner according to their target nuclei.

3. Morphology of BDA-labeled output cells in the neostriatum

We found that a large number of cells in the caudate nucleus and putamen were strongly BDA-labeled throughout the somata and dendrites. The photomicrographs in Figure 5A-D illustrate the morphological features of the output cells in the caudate nucleus labeled with BDA injections into the GP (A, B), EP (C) and SNR (D). The majority of the labeled output cells were multipolar in shape (A, C, D), the remaining being fusiform (B) and pyramidal. Multipolar cells had 4–8 primary (1^{st}-order) dendrites, whereas fusiform and pyramidal cells had 3-4. The range of soma diameters for the caudate output cells, irrespective of their shape, was 12-27 μm (long axis) X 6-17 μm (short axis). Their mean ± SEM diameter along the long X short axis was 17.7 ± 3.8 X 10.9 ± 2.7 μm (GP injection), 18.7 ± 3.2 X 11.5 ± 2.0 μm (EP) and 18.2 ± 3.2 X 11.8 ± 1.8 μm (SNR) (n=60 for each). There was no significant difference in the size of the output cells labeled with BDA injections into the GP, EP and SNR.

High magnification photomicrographs in Figure 5E and F illustrate parts of dendrites emerging from the soma shown in Figure A and B, respectively. The length of dendrites of these 2 cells was 150-250 μm. On these dendrites, a number of spine-like structures were located. The primary dendrites and the initial part of most secondary dendrites lacked spines. Generally, the number of spines increased as far as distal on the tertiary and above dendrites, but decreased at their most remote parts. Such organization of the dendritic trees was commonly observed between the output

cells labeled with BDA injections into GP, EP and SNR.

5-HT innervation to the neostriatal output cells and cholinergic interneurons

1. 5-HT innervation to the output cells projecting to the GP, EP and SNR

In the sections double stained for BDA and 5-HT immunoreactivity, 5-HT-immunopositive fibers (5-HT fibers) were distributed profusely throughout the rostrocaudal extent of the caudate nucleus and putamen, together with a great number of BDA-labeled cells. In the neostriatum, the majority of 5-HT fibers had fine calibers (diameter < 0.6 μm) with round varicosities. In all cats with BDA injections into the GP, EP and SNR, 5-HT fibers were distributed densely around the BDA-labeled cells.

The photomicrographs in Figure 6A-C show 3 BDA-labeled cells (brown) and 5-HT fibers (blue-black) in the caudate nucleus. Labeled cells were multipolar with a soma diameter of 15-20 μm. These cells extended 5-6 primary dendrites with distal (2^{nd}-4^{th} order) spiny dendrites. The labeled cell in Figure 6A extended its dendrites dorsally and ventrally, and the cells in Figure 6B-C extended their dendrites to all the directions. As shown in the photomicrographs A-C, 5-HT fibers formed a mesh-like plexus, and they were densely distributed around each of the labeled cells including both somatic and dendritic fields. The camera lucida drawings in Figure 6D-F show the distribution pattern of 5-HT fibers (black) and BDA-labeled cells (red). Some 5-HT fibers were closely apposed to soma and dendrites of the cells.

The high-magnification photomicrographs in Figure 7A-D illustrate BDA-labeled cells (brown) and 5-HT terminal fibers (blue-black) in the caudate nucleus. Many fine fibers with round varicosities were densely distributed around the labeled cells, and some fibers were closely apposed to the soma and/or dendrites. Single varicose 5-HT fibers were closely apposed to the soma of the labeled cells

(arrowheads), possibly forming putative synaptic contacts with the soma. Single 5-HT fibers indicated by arrows in C-D coursed along the margin of the cells forming putative synaptic contacts with both the soma and primary dendrites (arrowheads). Varicose 5-HT fibers were also closely apposed to the distal dendrites. The photomontages in Figure 8A-C illustrate 5-HT terminal fibers (blue-black) and distal dendrites (brown) of the labeled cells in the caudate nucleus. As shown in the photomicrographs, many 5-HT terminal fibers were densely distributed around distal dendrites with spines. A single 5-HT fiber shown in Figure 8A ran dorsomedially along a distal spiny dendrite and formed a few close appositions to the dendrite (arrowheads). This 5-HT fiber further ran dorsomedially, and then it was closely apposed to a distal spiny dendrite (white arrowhead), which originated from other cell.

Three 5-HT fibers shown in Figure 8B (upward arrows) ran dorsally and dorsomedially, and they were closely apposed to a single distal dendrite at three different sites (filled and open arrowheads). As shown in the inset high-magnification photomicrograph (B), the terminal fibers indicated by filled and open arrowheads had close appositions to the dendritic shaft and the spine, respectively. Figure 8C shows a single 5-HT fiber running ventromedially for a long distance (~ 250 μm). During its course, this fiber was closely apposed to three distal dendrites at five sites (filled and open arrowheads). These dendrites originated from the same cell. As shown in the inset photomicrograph, this fiber was closely apposed not only to the dendritic shaft (filled arrowhead) but also to the spine (open arrowhead).

2. 5-HT innervation to the cholinergic interneurons

In the sections double stained for ChAT and 5-HT immunoreactivities, we found that ChAT cells and 5-HT fibers were distributed throughout the rostrocaudal extent of the neostriatum. Similar to the results in our recent study (Okumura et al., in press), ChAT cells were multipolar with a soma diameter of 20-50 μm (long axis) X

10-30 μm (short axis), and their density was ~7-10 cells/mm^2 throughout the full rostrocaudal extent of the caudate nucleus and putamen.

The photomicrographs in Figure 9A-D show ChAT cells and 5-HT fibers observed in the caudate nucleus of a single double stained section. These ChAT cells were large-sized multipolar cells with 3-5 primary dendrites. As shown in Figure 9A-D, fine 5-HT fibers formed a mesh-like plexus throughout the dorsal (A, B), middle (C) and ventral (D) portions of the caudate nucleus, and some of them were distributed around ChAT cells. The density of 5-HT fibers was similar in the dorsal to middle portions (Fig. 9A-C), whereas the density was higher in the ventral portion (Fig. 9D) than others. The high-magnification photomicrographs in Figure 10A-D illustrate ChAT cells (dark) and 5-HT terminal fibers (black) in the caudate nucleus. The photomicrographs A and B show that single varicose 5-HT fibers ran along the margin of ChAT cells closely apposed to the soma (arrowheads). The photomicrographs C and D show that ChAT cells were often surrounded by several 5-HT fibers, which were closely apposed to soma and primary dendrite (arrowheads). In Figure 10D, a few large-sized varicosities (open arrowheads) were found on the cell in addition to small ones.

DISCUSSION

Topographical organization of striatal projection neurons to the GP, EP and SNR

There appears to be at least rough topographical organization in the corticostriatal connections (Selemon et al., 1985) and in the striatal efferents to the two segments of the globus pallidus (GP and EP) and the substantia nigra (Bunney and Aghajanian, 1976; Carpenter, 1984). In comparison to extensive studies relating to the corticostriatal organization (Alexander et al., 1986; Alexander and Crutcher, 1990), the organization of the striatal projections to the three target structures has not been fully understood. By using double-retrograde tracing method with rhodamine fluorescent latex microspheres (FM) in combination with either HRP or the fluorescent nuclear dye Diamidino Yellow (DY), Beckstead and Cruz (1986) studied the extent to which individual striatal neurons send collaterals to the GP, EP and SN in the cat brain. They found that SN- and EP-projecting output cells are distributed in common at all caudal levels of the caudate nucleus and putamen, and that the GP-projecting cells are largely absent at caudal levels of both striatal nuclei. They also found that the striatal cells which project to the three target structures overlap and intermingle extensively in most parts of the striatum. Their observations in the cat confirmed the discontinuous nature of the projection neuron clusters and the paucity of collateralized axons.

The major implication of the results obtained by Beckstead and Cruz (1986) was that striatal outputs to the GP, EP and SN appeared to come largely from different populations of neurons. The vast majority of striatal neurons did not appear to send collateral branches of their axons to more than one striatal target structure in contrast to the proposition that many striopallidal axons are collateral branches of strionigral fibers (Fox et al., 1975). In the striatum, output cells sending efferent projections to a common target area seemed to cluster together, without having simple relationship

between these clusters and the well-established mosaic pattern of different neurotransmitter system markers in the striatum (Graybiel et al., 1981; Herkenham and Pert, 1981). Beckstead and Cruz (1986) also suggested that the striatal region in which cells labeled by EP and SN deposits are most commonly found (dorsal part of the head of the caudate nucleus) corresponds to the region where the substance-P (SP)-containing cells reside. They also suggested that the striatal region in which cells labeled by GP deposit (ventral part of the caudate head and rostral putamen) corresponds to the region where opioid-containing cells reside.

In this study, we found a general tendency that GP-projecting cells to occur at highest density in the dorsal part of the caudate body, and that EP-projecting neurons to occur at highest density in the dorsal part of the caudate head, whereas SNR-projecting cells had their highest density in a more ventral portion of the head and body of the caudate nucleus. It was interesting that at those A-P levels where the density of GP-, EP- and SNR-projecting cells are highest, the density of cells in the putamen tended to be the highest. Such a tendency was maintained regardless of the volume of BDA injections into each of the GP, EP and SNR. At this stage of our study, it is difficult to speculate why our results and those by Beckstead and Cruz (1986) are different with regard to the topographical organization of the retrogradely labeled cells in the striatum. This may be due to the usage of different type of neural tracers and injection technique. In the study by Beckstead and Cruz (1986), injected DY into the target nuclei was concentrated in the cell nucleus rather than perikaryon where the FM accumulates. In our study, injected DB into the GP, EP and SN was retrogradely transported not only to the perikaryon but also to the primary and distal dendrites. Spines were also detectable in the remote dendrites, clearly indicated that GP-, EP- and SNR-projection neurons are spiny small to medium sized cells in agreement with the previous observations (Grofova, 1975).

Serotonergic innervation to the output neurons and interneurons in the neostriatum

The ascending serotonergic pathway originates near-exclusively from the dorsal raphe nucleus, which is the major source of the raphe-striatal pathway (Azmitia and Segal, 1978; Moore et al., 1978; Becquet et al., 1990). Previous 5-HT immunohistochemical studies have shown that 5-HT fibers were distributed densely in the neostriatum, forming fine and widespread networks, in the rat (Soghomonian et al., 1987), cat (Mori et al., 1985) and monkey (Pasik and Pasik, 1982). In these species, 5-HT fibers were particularly abundant in the ventromedial region of the neostriatum (Sano et al., 1982). Our recent study in the cat (Okumura et al., in press) showed essentially the same topographic distribution of 5-HT fibers in the neostriatum as those reported by Mori et al. (1985) and Sano et al. (1982). In the patch and matrix compartments of the neostriatum, we also found homogeneous distribtution of 5-HT fibers. Our findings suggest that 5-HT fibers might innervate both the output projection cells and cholinergic interneurons of the neostriatum, because these cells are distributed in both compartments throughout the whole extent of the caudate nucleus although they have some heterogeneous distribution (Gerfen, 1992; Kubota and Kawaguchi, 1993).

At the fine morphological level, only a few reports have examined the serotonergic neostriatal innervation in detail in the rat (Arluson and De La Manche, 1980; Soghomonian et al., 1989), cat (Calas et al., 1976) and monkey (Pasik and Pasik, 1982). In the electron microscopic study of the rat neostriatum, Soghomonian et al. (1989) reported that, although only 10-13% of 5-HT varicosities exhibited a synaptic junction, junctional 5-HT terminals synapsed exclusively, and with equal frequency, on dendritic spines or shafts, almost always with asymmetrical membrane

differentiations. They further reported that, whether or not exhibiting a synaptic contact, the 5-HT labeled terminals were found directly apposed to a variety of structures comprising other axon terminals, dendritic spines and branches, and somata. In the present study, we investigated 5-HT innervation to the output cells and cholinergic interneurons in the cat neostriatum. Using a neural tracer, BDA, the output cells projecting to the GP, EP and SNR were precisely identified including their fine morphology such as soma, dendrites and spines. 5-HT varicose fibers were densely distributed around all types of identified output cells projecting to the GP, EP and SNR, and a part of the fibers were closely apposed to their soma and dendrites. In accordance with Soghomonian et al. findings (1989), 5-HT varicosities were closely apposed to both dendritic spines and shafts on the distal dendrites in addition to somata and proximal dendrites. Such various appositional features of 5-HT varicosities suggest that the effects of 5-HT in the neostriatum might be exerted upon a multiplicity of cellular target sites throughout all types of the identified output cells. Furthermore, considering that 5-HT fibers were closely apposed to the soma and dendrites of cholinergic interneurons, the raphe-striatal 5-HT system as a whole may control the intrinsic activity of the neostriatum together with the output patterns to the target nuclei.

Functional role of the serotonergic innervation of cholinergic interneurons and output projection neurons

Many studies suggest that 5-HT plays inhibitory and/or excitatory roles in the regulation of skeletal and visceral motor functions. Green et al. (1976) and Herman (1975) found that acute intraventricular injections of 5-HT resulted in a transient decrease in spontaneous locomotor activity in rats and mice, respectively. Studies with a precursor of 5-HT (such as tryptophan, TP or 5-hydroxytryptophan, 5-HTP),

however, yielded results that varied with the condition of the experiments. Increased behavioral activity followed the administration of 5-HT in animals which were pre-treated with drugs that further increase 5-HT in the CNS. The "hyperactivity" (serotonin syndrome) was observed in rats and guinea pigs which had been given TP following an inhibitor of monoamine oxidase (MAO) (Grahame-Smith, 1971; Deakin and Green, 1978; Chadwick et al., 1978; Volkman et al., 1978). Similarly, the syndrome was seen in rodents following administration of drugs that block the neuronal reuptake of 5-HT, provided the animals was pretreated with MAO inhibitor (Modigh, 1973; Holman and Seagraves, 1976). A variety of studies suggested that both presynaptic and postsynaptic mechanisms are involved in the expression of either inhibitory or excitatory effects of 5-HT on motor behaviors (Gerson and Baldessarini, 1980). Trulson et al. (1976) suggested that behavioral syndrome might in part reflect loss or impairment of presynaptic high-affinity reuptake into 5-HT containing cells, with little or no concomitant change in the sensitivity of the postsynaptic receptors. Since drugs that stimulate postsynaptic 5-HT receptor produced abnormal motor responses, Stewart et al. (1979) suggested that activation of 5-HT receptors is invovled and that serotonin syndrome is primarily of the postsynaptic type.

Studies by Glennom (1990), Hartig et al. (1990) and Peroutka et al. (1990) suggested that physiological effects of serotonergic transmission in the CNS are mediated by several 5-HT receptor subtypes, designated 5-HT1, 5-HT2, 5-HT3 and 5-HT4. Hoyer et al. (1994) further described that serotonin receptors form a large family of 14 separate cloned genes in mammals. Several of these receptors have been shown to be expressed in the striatum or nucleus accumbens, where they presumably respond to serotonergic input from the dorsal raphe nucleus (Ward and Dorsa, 1996). Serotonin receptors, 5-HT1B (Boschert et al., 1994; Bruinvels et al., 1994), 5-HT1E (Bruinvels et al., 1994), 5-HT2A and 5-HT2C (Mengod et al., 1990; Pompeiano et al., 1994), 5-HT4 (Jakeman et al., 1994; Gerald et al., 1995), and 5-HT6

(Ward et al., 1995) have been demonstrated to express in the striatum. Morilak and Ciaranello (1993) studied the distribution of mRNAs of the three serotonin receptors (5-HT2A, 5-HT2C, and 5HT-6) in the striatum, together with the distribution of three neuropeptides (enkephalin, substance P, dynorphin). They found that all the receptors were colocalized with all three of the neuropeptides. None of the serotonin receptors showed preferential colocalization in striopallidal (enkephalin containing), or strionigral (substance P or dynorphin containing) cells. Recent study by Cornea-Hebert et al. (1999) demonstrated that most of the striatal medium spiny neurons appeared to be 5-HT2A immunostained, as well as some larger neuronal soma/dendrites, presumably interneurons.

In the present study, we demonstrated clearly that both the somata and dendrites of cholinergic interneurons, and those of striopallidal and strionigral pojections neurons are finely innervated by serotonergic fibers and varicosities. Previous studies by Izzo and Bolam (1988) demonstrated that cholinergic interneurons distribute their terminal fibers around the somata and proximal dendrites of the output projection neurons. At this stage of our studies, it is difficult to speculate whether serotonergic innervation to cholinergic and output projections neurons in the neostriatum is related to inhibitory or excitatory actions of 5-HT on them because a number of 5-HT receptors may be present in the output projection neurons. In many regions in the central nervous system where 5-HT1A and 5-HT2 receptors have been found to co-extensive, including the neocortex, periaquaductal grey, and pontine reticular formation, they exert opposing influences, with 5-HT1A receptors mediating inhibition and 5-HT2 receptors eliciting excitation (Araneda and Andrade, 1991; Aghajanian and Marek, 1997). Thus 5-HT2 receptors may elicit an excitatory effect on cholinergic interneurons. Recent study by Morilak and Ciaranello (1993) in rats showed, however, little colocalization of 5-HT2 and ChAT immunoreactivity in neurons of the striatum.

It is interesting to note here that the striatal serotonin system is fundamentally different from the striatal dopamine system. The serotonin receptor system does not share the characteristics of dopamine receptor system (Ward and Dorsa, 1996). We think that, in understanding the physiological roles played by serotonin, the fundamental differences in distribution of the 5-HT receptors within the cholinergic interneurons and output projection neurons need to be elucidated together with better understanding of dopamine and Ach receptors within them.

REFERENCES

Aghajanian GK, Marek GJ. 1997. Serotonin induces excitatory postsynaptic potentials in apical dendrites of neocortical pyramidal cells. Neuropharmacology 36: 589-599.

Albin RL, Young AB, Penney JB. 1989. The functional anatomy of basal ganglia disorders. Trends Neurosci 12: 366-375.

Alexander GE, Crutcher MD. 1990. Functional architecture of basal ganglia circuits: neural substrates of parallel processing. Trends Neurosci 13: 266-271

Alexander GE, DeLong MR, Strick PL. 1986. Parallel organization of functionally segregated circuits linking basal ganglia and cortex. Annu Rev Neurosci 9: 357-381.

Araneda R, Andrade R. 1991. 5-Hydroxytryptamine2 and 5-hydroxytryptamine 1A receptors mediate opposing responses on membrane excitability in rat association cortex. Neuroscience 40: 399-412.

Arluison M, De La Manche IS. 1980. High-resolution radioautographic study of the serotonin innervation of the rat corpus striatum after intraventricular administration of [3H]5-hydroxytryptamine. Neuroscience 5: 229-240.

Azmitia EC, Segal M 1978. An autoradiographic analysis of the differential ascending projections of the dorsal and median raphe nuclei in the rat. J Comp Neurol 179: 641-67.

Beckstead RM, Cruz CJ. 1986. Striatal axons to the globus pallidus, entopeduncular nucleus and substantia nigra come mainly from separate cell populations in cat. Neuroscience 19: 147-158.

Becquet D, Faudon M, Hery F. 1990. The role of serotonin release and autoreceptors in the dorsalis raphe nucleus in the control of serotonin release in the cat caudate nucleus. Neuroscience 39: 639-647.

Berman A, Jones EG. 1982. The thalamus and basal telencephalon of the cat. Madison,

The university of wisconsin press.

Boschert U, Amara DA, Segu L, Hen R. 1994. The mouse 5-hydroxytryptamine1B receptor is localized predominantly on axon terminals. Neuroscience 58: 167-182.

Bruinvels AT, Landwehrmeyer B, Gustafson EL, Durkin MM, Mengod G, Branchek TA, Hoyer D, Palacios JM. 1994. Localization of 5-HT1B, 5-HT1D alpha, 5-HT1E and 5-HT1F receptor messenger RNA in rodent and primate brain. Neuropharmacology 33: 367-386.

Bunney BS, Aghajanian GK. 1976. The precise localization of nigral afferents in the rat as determined by a retrograde tracing technique. Brain Res 117: 423-435

Calas A, Besson MJ, Gaughy C, Alonso G, Glowinski J, Cheramy A. 1976. Radioautographic study of in vivo incorporation of 3H-monoamines in the cat caudate nucleus: identification of serotoninergic fibers. Brain Res 118: 1-13.

Carey MP, Diewald LM, Esposito FJ, Pellicano MP, Gironi Carnevale UA Sergeant JA, Papa M, Sadile AG. 1998. Differential distribution, affinity and plasticity of dopamine D-1 and D-2 receptors in the target sites of the mesolimbic system in an animal model of ADHD. Behav Brain Res 94: 173-185.

Carpenter MB. 1984. Interconnection between the corpus striatum and brain stem nuclei. In: McKenzie JS, Kemm RE, Wilcock LN, editors: The Basal Ganglia : Structure and Function (Advances in Behavioral Biology, Vol 27): Plenum Pub Corp. pp.1-67.

Chadwick D, Hallett M, Jenner P, Marsden CD. 1978. 5-hydroxytryptophan-induced myoclonus in guinea pigs. A physiological and pharmacological investigations. Journal Of The Neurol Sci 35: 157-165.

Chase TN. 1974. Serotonergic mechanisms and extrapyramidal function in man. Adv Neurol 5: 31-39.

Cornea-Hébert V, Riad M, Wu C, Singh SK, Descarries L. 1999. Cellular and subcellular distribution of the serotonin 5-HT2A receptor in the central nervous

system of adult rat. J Comp Neurol 409: 187-209.

Cote SL, Silva RD, Cuello AC. 1993. Current protocol for light microscopy immunocytochemistry. In: A Cuello, editor: Immunohistochemistry II. West Sussex: Jhon Wiley & Sons Ltd. pp.148-167.

Deakin JF, Green AR. 1978. The effects of putative 5-hydroxytryptamine antagonists on the behaviour produced by administration of tranylcypromine and L-tryptophan or tranylcypromine and L-DOPA to rats. Br J Pharmacol 64: 201-209.

Fox CA, Rafols JA, Cowan WM. 1975. Computer measurements of axis cylinder diameters of radial fibers and "comb" bundle fibers. J Comp Neurol 159 201-223

Gainetdinov RR, Wetsel WC, Jones SR, Levin ED, Jaber M, Caron MG. 1999. Role of serotonin in the paradoxical calming effect of psychostimulants on hyperactivity. Science 283: 397-401.

Gerald C, Adham N, Kao HT, Olsen MA, Laz TM, Schechter LE, Bard JA, Vaysse PJ, Hartig PR, Branchek TA, et al.. 1995. The 5-HT4 receptor: molecular cloning and pharmacological characterization of two splice variants. Embo J 14: 2806-2815.

Gerfen CR. 1992. The neostriatal mosaic: multiple levels of compartmental organization in the basal ganglia. Annu Rev Neurosci 15: 285-320.

Gerson SC, Baldessarini RJ. 1980. Motor effects of serotonin in the central nervous system. Life Sci 27: 1435-1451.

Glennon, RA. 1990. Serotonin receptors: clinical implications. Neurosci Biobehav Rev 14: 35-47.

Grace AA, Llinás R. 1985. Morphological artifacts induced in intracellularly stained neurons by dehydration: circumvention using rapid dimethyl sulfoxide clearing. Neuroscience 16: 461-475.

Grahame-Smith DG. 1971. Studies in vivo on the relationship between brain tryptophan, brain 5-HT synthesis and hyperactivity in rats treated with a monoamine oxidase inhibitor and L-tryptophan. J Neurochem 18: 1053-1066.

Graybiel AM, Ragsdale CW., Jr. 1978. Histochemically distinct compartments in the striatum of human, monkeys, and cat demonstrated by acetylthiocholinesterase staining. Proc Natl Acad Sci U S A 75: 5723-5726.

Graybiel AM, Ragsdale CW., Jr., Yoneoka ES, Elde RP. 1981. An immunohistochemical study of enkephalins and other neuropeptides in the striatum of the cat with evidence that the opiate peptides are arranged to form mosaic patterns in register with the striosomal compartments visible by acetylcholinesterase staining. Neuroscience 6: 377-397.

Green RA, Gillin JC, Wyatt RJ. 1976. The inhibitory effect of intraventricular administration of serotonin on spontaneous motor activity of rats. Psychopharmacology (Berl) 51: 81-84.

Grofová I. 1975. The identification of striatal and pallidal neurons projecting to substantia nigra. An experimental study by means of retrograde axonal transport of horseradish peroxidase. Brain Res 91: 286-291.

Hartig P, Kao HT, Macchi M, Adham N, Zgombick J, Weinshank R, Branchek T. 1990. The molecular biology of serotonin receptors. An overview. Neuropsychopharmacology 3: 335-347.

Herkenham M, Pert CB. 1981. Mosaic distribution of opiate receptors, parafascicular projections and acetylcholinesterase in rat striatum. Nature 291: 415-418.

Herman ZS. 1975. Behavioural changes induced in conscious mice by intracerebroventricular injection of catecholamines, acetylcholine and 5-hydroxytryptamine. Br J Pharmacol 55: 351-358.

Holman RB, Seagraves E, Elliott GR, Barchas JD. 1976. Stereotyped hyperactivity in rats treated with tranylcypromine and specific inhibitors of 5-HT reuptake. Behavioral Biology 16: 507-514.

Hoyer D, Clarke DE, Fozard JR, Hartig PR, Martin GR, Mylecharane EJ, Saxena, PR, Humphrey PP. 1994. International Union of Pharmacology classification of

receptors for 5-hydroxytryptamine (Serotonin). Pharmacol Rev 46: 157-203.

Izzo PN, Bolam JP. 1988. Cholinergic synaptic input to different parts of spiny striatonigral neurons in the rat. J Comp Neurol 269: 219-234

Jakeman LB, To ZP, Eglen RM, Wong EH, Bonhaus DW. 1994. Quantitative autoradiography of 5-HT4 receptors in brains of three species using two structurally distinct radioligands, [3H]GR113808 and [3H]BIMU-1. Neuropharmacology 33: 1027-1038.

Kubota Y, Kawaguchi Y. 1993. Spatial distributions of chemically identified intrinsic neurons in relation to patch and matrix compartments of rat neostriatum. J Comp Neurol 332:499-513.

Kita H, Kitai ST. 1988. Glutamate decarboxylase immunoreactive neurons in rat neostriatum: their morphological types and populations. Brain Res 447: 346-352.

Mengod G, Pompeiano M, Martínez-Mir MI, Palacios JM. 1990. Localization of the mRNA for the 5-HT2 receptor by in situ hybridization histochemistry. Correlation with the distribution of receptor sites. Brain Res 524: 139-143.

Modigh K. 1973. Effects of chlorimipramine and protriptyline on the hyperactivity induced by 5-hydroxytryptophan after peripheral decarboxylase inhibition in mice. J Neural Transm 34: 101-109.

Moore RY, Halaris AE, Jones BE. 1978. Serotonin neurons of the midbrain raphe: ascending projections. J Comp Neurol 180: 417-438.

Mori S. Ueda S, Yamada H, Takino T, Sano, Y. 1985. Immunohistochemical demonstration of serotonin nerve fibers in the corpus striatum of the rat, cat and monkey. Anat Embryol (Berl) 173: 1-5.

Morilak DA, Ciaranello RD. 1993. 5-HT2 receptor immunoreactivity on cholinergic neurons of the pontomesencephalic tegmentum shown by double immunofluorescence. Brain Res 627: 49-54.

Okumura T, Dobolyi A, Matsuyama K, Mori S. 1999a. Cholinergic and serotonergic

interactions in the caudate nucleus of the cat: Relation to behavioral control. Neurosci Res 23: S197.

Okumura T, Dobolyi A, Matsuyama K, Kakigi R, Mori S. 1999b. Cholinergic and serotonergic interactions in the caudate nucleus in relation to behavioral control in cats. Soc Neurosci Abstr 25: 1155.

Okumura T, Dobolyi A, Matsuyama K, Mori F, Mori S. The cat neostriatum: relative distribution of cholinergic neurons vs. serotonergic fibers. Brain Dev: In press.

Pasik T, Pasik P. 1982. Serotoninergic afferents in the monkey neostriatum. Acta Biol Acad Sci Hung 33: 277-288.

Peroutka SJ, Schmidt AW, Sleight AJ, Harrington MA. 1990. Serotonin receptor families in the central nervous system: an overview. Ann N Y Acad Sci 600: 104-112; discussion 113.

Pompeiano M, Palacios JM, Mengod G. 1994. Distribution of the serotonin 5-HT2 receptor family mRNAs: comparison between 5-HT2A and 5-HT2C receptors. Brain Res. Molecular Brain Research 23: 163-178.

Russell V, de Villiers A, Sagvolden T, Lamm M, Taljaard J. 1998. Differences between electrically-, ritalin- and D-amphetamine-stimulated release of [3H]dopamine from brain slices suggest impaired vesicular storage of dopamine in an animal model of Attention-Deficit Hyperactivity Disorder. Behav Brain Res 94: 163-171.

Sano Y, Takeuchi Y, Kimura H, Goto M, Kawata M, Kojima M, Matsuura T, Ueda S, Yamada H. 1982. Immunohistochemical studies on the processes of serotonin neurons and their ramification in the central nervous system--with regard to the possibility of the existence of Golgi's rete nervosa diffusa. Arch Histol Jpn 45: 305-316

Selemon LD, Goldman-Rakic PS. 1985. Longitudinal topography and interdigitation of corticostriatal projections in the rhesus monkey. J Neurosci 5: 776-794

Soghomonian JJ, Doucet G, Descarries L. 1987. Serotonin innervation in adult rat neostriatum. I. Quantified regional distribution. Brain Res 425: 85-100.

Soghomonian JJ, Descarries L, Watkins KC. 1989. Serotonin innervation in adult rat neostriatum. II. Ultrastructural features: a radioautographic and immunocytochemical study. Brain Res 481: 67-86.

Steinbusch HW, Verhofstad AA, Joosten HW. 1978. Localization of serotonin in the central nervous system by immunohistochemistry: description of a specific and sensitive technique and some applications. Neuroscience 3: 811-819.

Steinbusch HW, Nieuwenhuys R, Verhofstad AA, Van der Kooy D. 1981. The nucleus raphe dorsalis of the rat and its projection upon the caudatoputamen. A combined cytoarchitectonic, immunohistochemical and retrograde transport study. J Physiol (Paris) 77: 157-174.

Stewart RM, Campbell A, Sperk G, Baldessarini RJ. 1979. Receptor mechanisms in increased sensitivity to serotonin agonists after dihydroxytryptamine shown by electronic monitoring of muscle twitches in the rat. Psychopharmacology (Berl) 60: 281-289.

Takeuchi Y, Kimura H, Sano Y. 1982. Immunohistochemical demonstration of the distribution of serotonin neurons in the brainstem of the rat and cat. Cell Tissue Res 224:247-267.

Trulson ME, Eubanks EE, Jacobs BL. 1976. Behavioral evidence for supersensitivity following destruction of central serotonergic nerve terminals by 5,7-dihydroxytryptamine. J Pharmacol Exp Ther 198: 23-32.

Volkman PH, Lorens SA, Kindel GH, Ginos JZ. 1978. L-5-Hydroxytryptophan-induced myoclonus in guinea pigs: a model for the study of central serotonin-dopamine interactions. Neuropharmacology 17: 947-955.

Ward RP, Hamblin MW, Lachowicz JE, Hoffman BJ, Sibley DR, Dorsa DM. 1995. Localization of serotonin subtype 6 receptor messenger RNA in the rat brain by in

situ hybridization histochemistry. Neuroscience 64: 1105-1011.

Ward RP, Dorsa DM. 1996. Colocalization of serotonin receptor subtypes 5-HT2A, 5-HT2C, and 5-HT6 with neuropeptides in rat striatum. J Comp Neurol 370: 405-414.

FIGURE LEGENDS

Figure 1. Representative transverse-plane photomicrographs and camera lucida drawings of biotinylated dextran amine (BDA) injection sites in the globus pallidus (GP) at Horsley Clark coordinate A13.2 (**A**), the entopeduncular nucleus (EP) at A11.5 (**B**) and the substantia nigra pars reticulata (SNR) at A5.1 (**C**). A dark stained area indicated by a thick arrow in each photomicrograph corresponds to a center region of the BDA injection zone. In these examples, 0.3 μl of 20 % BDA was injected at the middle portion of each nucleus. On each lower drawing, the brain structures observed on each photomicrograph were illustrated using a camera lucida. On these drawings, the hatched areas indicate BDA diffusion areas. Abbreviations: AMG, amygdala; CA, caudate nucleus; CL, claustrum; EP, entopeduncular nucleus; FTC, central tegmental field; GP, globus pallidus; IC, internal capsule; LGN, lateral geniculate nucleus; LV, lateral ventricle; MGN, medial geniculate nucleus; OT, optic tract; PAG, periaqueductal gray; PP, pes peduncli; PT, pretectal nucleus; PU, putamen; R, red nucleus; SNL, substantia nigra, lateral division; SNR, substantia nigra pars reticulata; TH, thalamus; 3N, oculomotor nerve. Scale bars = 1 mm for all photomicrographs and drawings.

Figure 2. Low-magnification photomicrographs of representative distribution areas of retrogradely labeled cells in the caudate nucleus after BDA injections into the GP (**A**), EP (**B**) and SNR (**C**). The photomicrographs A, B and C were taken at levels A14.9, 16.4 and 14.9, respectively. BDA-labeled output cells were shown as dark stained particles. Dark stained areas in A is the region where labeled cells were highly concentrated. Asterisks (*) indicate the regions where few labeled cells were located in the aggregation area of the cells. The BDA injection areas of these examples A, B and C are shown on photomicrographs A, B and C in Figure 1, respectively. Abbreviations are the same as those used in Figure 1. Scale bar = 0.5

mm for A-C.

Figure 3. Rostrocaudal distribution pattern of retrogradely labeled output cells in the caudate nucleus and putamen at levels A19.4-12.9 after 0.3 μl BDA injections into the GP (**A**), EP (**B**) and SNR (**C**). On each drawing, locations of labeled cells observed on a single transverse section at each level are plotted by dots. The numbers of labeled cells at A19.4-12.9 in the caudate nucleus were 3, 48, 618, 1663, 1419 and 107 (A), 65, 337, 559, 272, 84 and 0 (B), and 54, 149, 605, 701, 415 and 47 (C), and those in the putamen were 0, 0, 17, 60, 87, 25 (A), 2, 35, 138, 50, 18 and 21 (B), and 1, 3, 243, 84, 69 and 21 (C). The plots and drawings at levels A14.9 in A, A16.4 in B and A14.9 in C were made from the same sections as shown in Figure 2A-C, respectively. The BDA injection area of the cats in A-C is shown in Figure 1A-C, respectively. Abbreviations are the same as those used in Figure 1. Scale bar = 2 mm for all drawings.

Figure 4. Distribution pattern of retrogradely labeled output cells in representative transverse planes at levels A14.5 (**A**), A16.4 (**B**) and A14.0 (**C**) of the cats with 0.15 μl BDA injection into the GP, EP and SNR, respectively. On each drawing, locations of the labeled cells observed on a single section are plotted by dots. The numbers of the cells in A-C were 1043, 920 and 247 in the caudate nucleus, and 52, 158 and 36 in the putamen, respectively. Abbreviations are the same as those used in Figure 1. Scale bars = 1 mm for A-C.

Figure 5. **A-D:** Photomicrographs of representative BDA-labeled output cells in the caudate nucleus. These cells were labeled after the injection into the GP (A, B), EP (B) and SNR (C). All photomicrographs were taken from sections made from the animals shown in Figures 1-3. **E-F:** High-magnification photomicrograph of

dendrites and spines emerging from labeled cell soma. Photomicrographs E and F were taken from the areas indicated by squares in A and B, respectively. Scale bar = 25 μm for A-D; 10 μm for E-F.

Figure 6. **A-C:** Photomicrographs of BDA-labeled output cells and 5-HT immunopositive fibers in the caudate nucleus. Each photomicrograph A-C was taken from a single section of the cat with the injection into the GP, EP and SNR, respectively. In these sections double stained for BDA and 5-HT-immunoreactivity, BDA-labeled cells and 5-HT-positive fibers are seen as brown and blue-black, respectively. The dendrites indicated by arrows in A and C are further illustrated in Figure 8A and C, respectively. **D-F:** Camera lucida drawings of BDA-labeled cells and 5-HT immunopositive fibers in the caudate nucleus. The drawings D-F was made from the same region shown in the photomicrographs A-C, respectively. In the drawings, BDA-labeled somata and dendrites are shown by red, and 5-HT fibers are shown by black. Arrowheads indicate the somata of the labeled cells. Scale bar = 30 μm for all photomicrographs and drawings.

Figure 7. Photomontages of BDA-labeled output cells and 5-HT-immunopositive fibers in the caudate nucleus. These photomontages were made from 3 photomicrograph taken from single double stained sections of the cats with the injection into the GP (**A**), EP (**B**, **C**) and SNR (**D**). Arrowheads indicate varicose 5-HT-positive fibers (blue-black) forming putative synaptic contacts with the soma and primary dendrites (brown) of the labeled cells. The cell shown in C corresponds to that in Figure 6B. Scale bar = 10 μm for A-D.

Figure 8. Photomontages of dendrites emerging from BDA-labeled output cells and 5-HT-immunopositive fibers in the caudate nucleus. These photomontages were

made from 3-5 photomicrographs taken from single double stained sections of the cats with BDA injection into the GP (**A**), EP (**B**) and SNR (**C**). All types of arrowheads indicate varicose 5-HT-positive fibers (blue-black) forming putative synaptic contacts with distal dendrites (brown), and thin arrows indicate the direction of 5-HT fibers. The dendrites in A and C emerged from the cell soma shown in Figure 6A and C, respectively. The areas encircled by dotted squares in B and C are further illustrated on the inset photomicrographs at a higher-magnification. Scale bar = 15 μm for A-C; 5 μm for the insets in B-C.

Figure 9. Photomicrographs of choline acetyltransferase (ChAT)-immunopositive interneurons and 5-HT-immunopositive fibers in the caudate nucleus at level A16.4. This section was double stained for ChAT- and 5-HT-immunoreactivities. The photomicrographs were taken from the dorsolateral (**A**), dorsomedial (**B**), middle (**C**) and ventral (**D**) portions of the caudate nucleus in the same section, respectively. In the photomicrographs, ChAT cells were seen as dark-stained cells indicated by arrowheads, and 5-HT fibers were seen as black-stained fine varicose fibers. Scale bar = 40 μm for A-D.

Figure 10. High-magnification photomicrographs of ChAT-immunopositive interneurons and 5-HT-immunopositive fibers in the caudate nucleus. In the photomicrographs, ChAT-positive cells and 5-HT-positive fibers are seen as dark-stained cells and black-stained fine varicose fibers, respectively. Arrowheads indicate varicose 5-HT-positive fibers forming putative synaptic contacts with the somata and/or proximal dendrites of ChAT-positive cells. Scale bar = 10 μm for A-D.

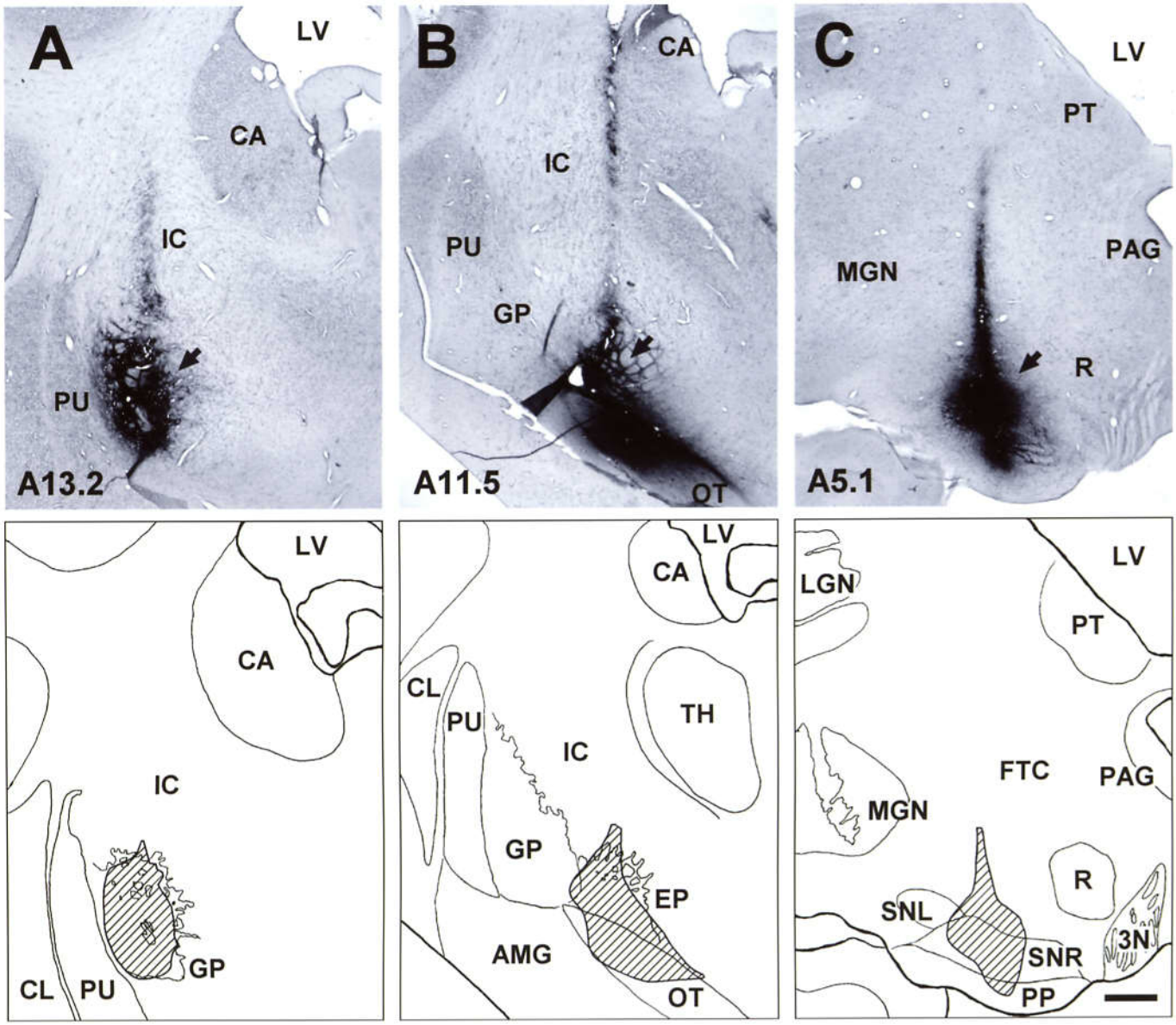
A
LV
CA
IC
PU
A13.2
B
CA
IC
PU
GP
A11.5
OT
C
LV
PT
PAG
MGN
R
A5.1
LV
CA
IC
CL
PU
GP
LV
CA
CL
PU
IC
TH
GP
EP
AMG
OT
LV
LGN
PT
FTC
PAG
MGN
R
SNL
SNR
3N
PP

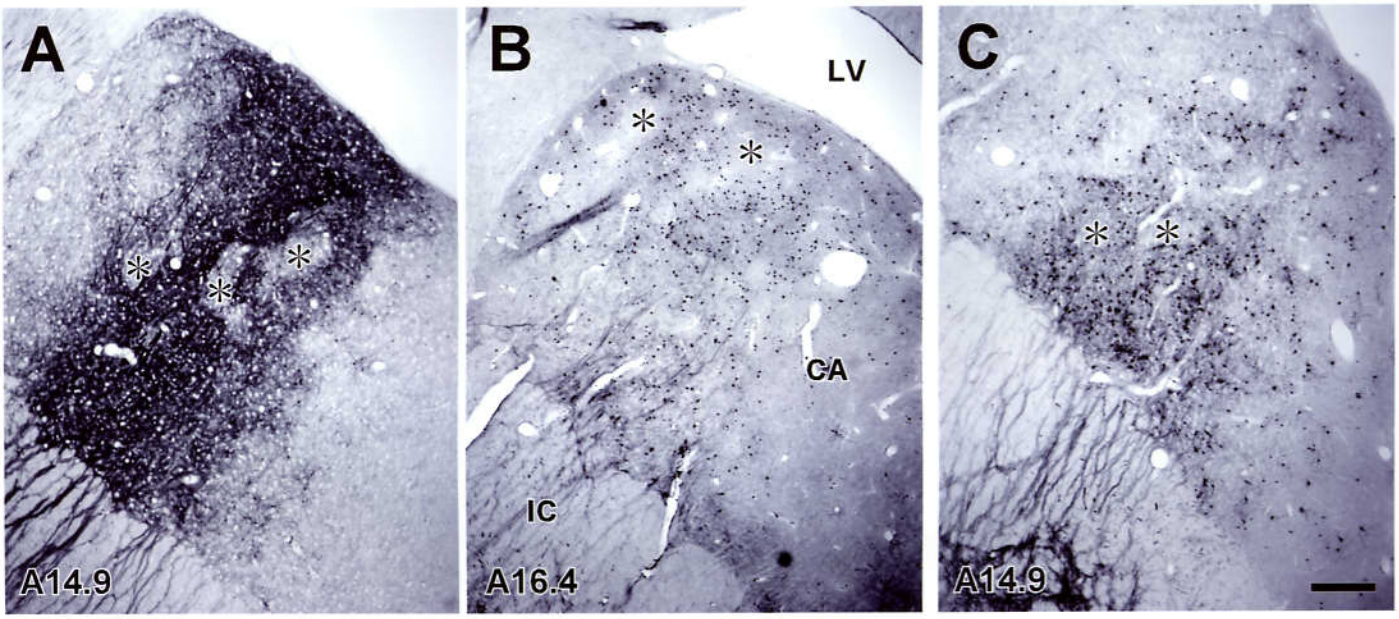
A
A14.9
B
LV
CA
IC
A16.4
C
A14.9

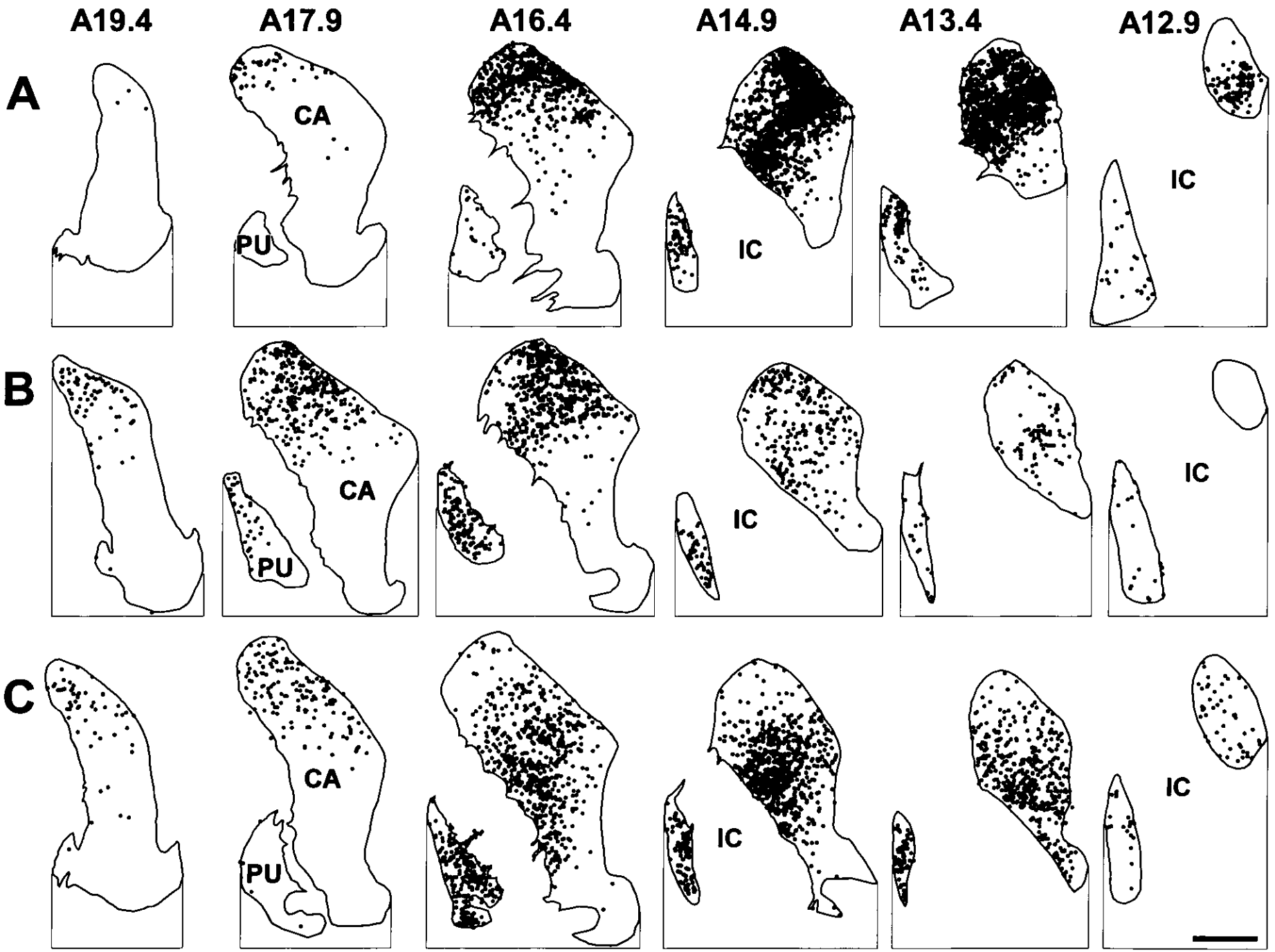
A19.4
A17.9
A16.4
A14.9
A13.4
A12.9
A
B
C
CA
PU
IC
IC
IC
CA
PU
IC
IC
IC
CA
PU
IC
IC

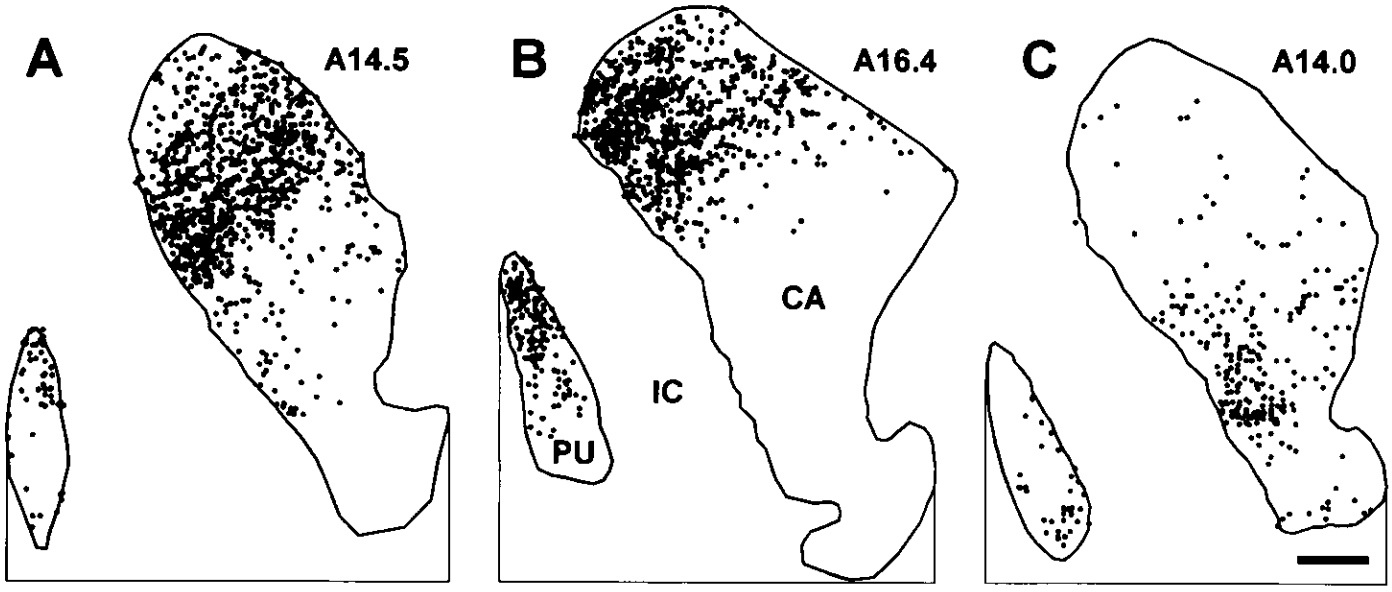
A
A14.5
B
A16.4
CA
IC
PU
C
A14.0

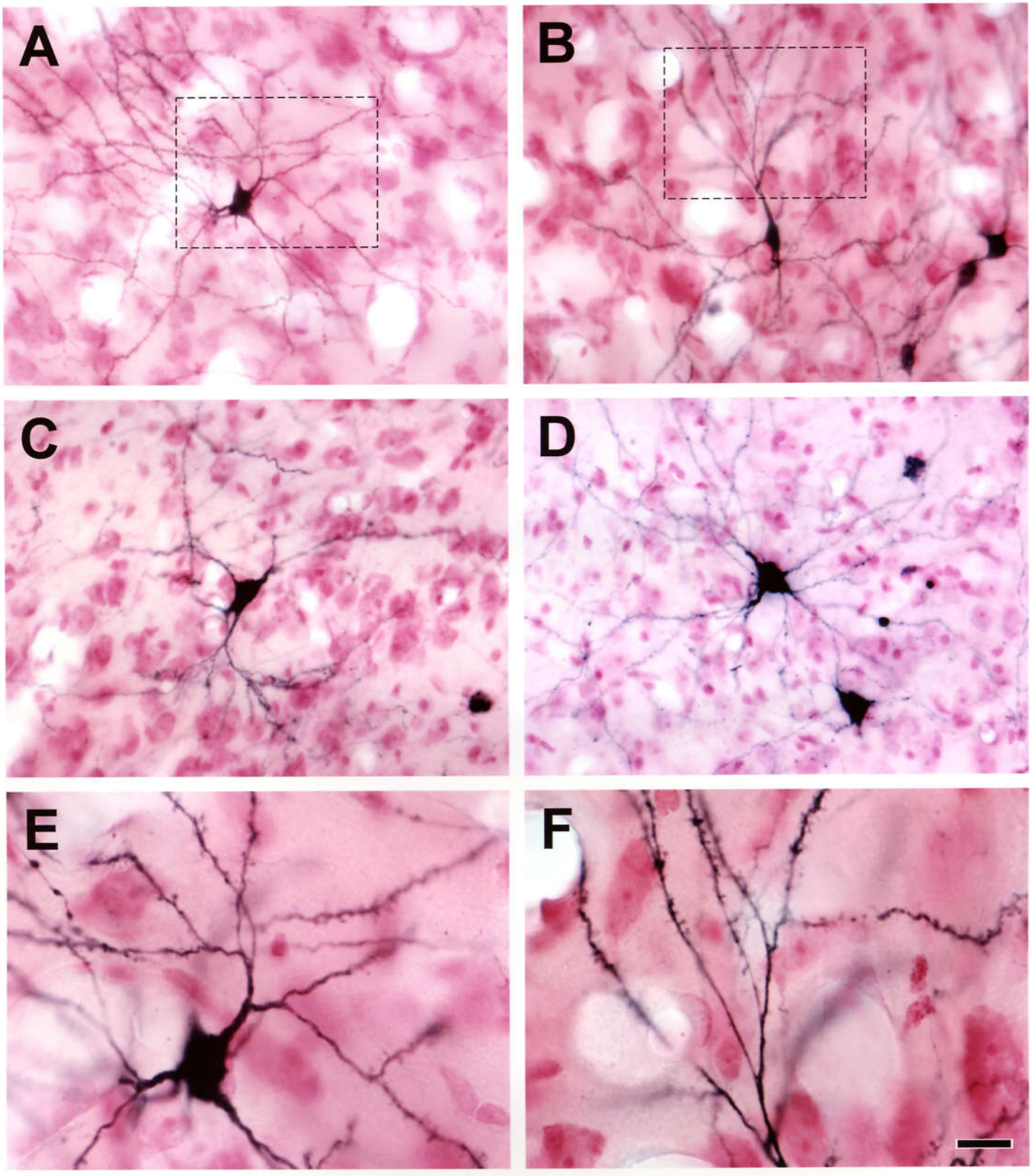
A
B
C
D
E
F

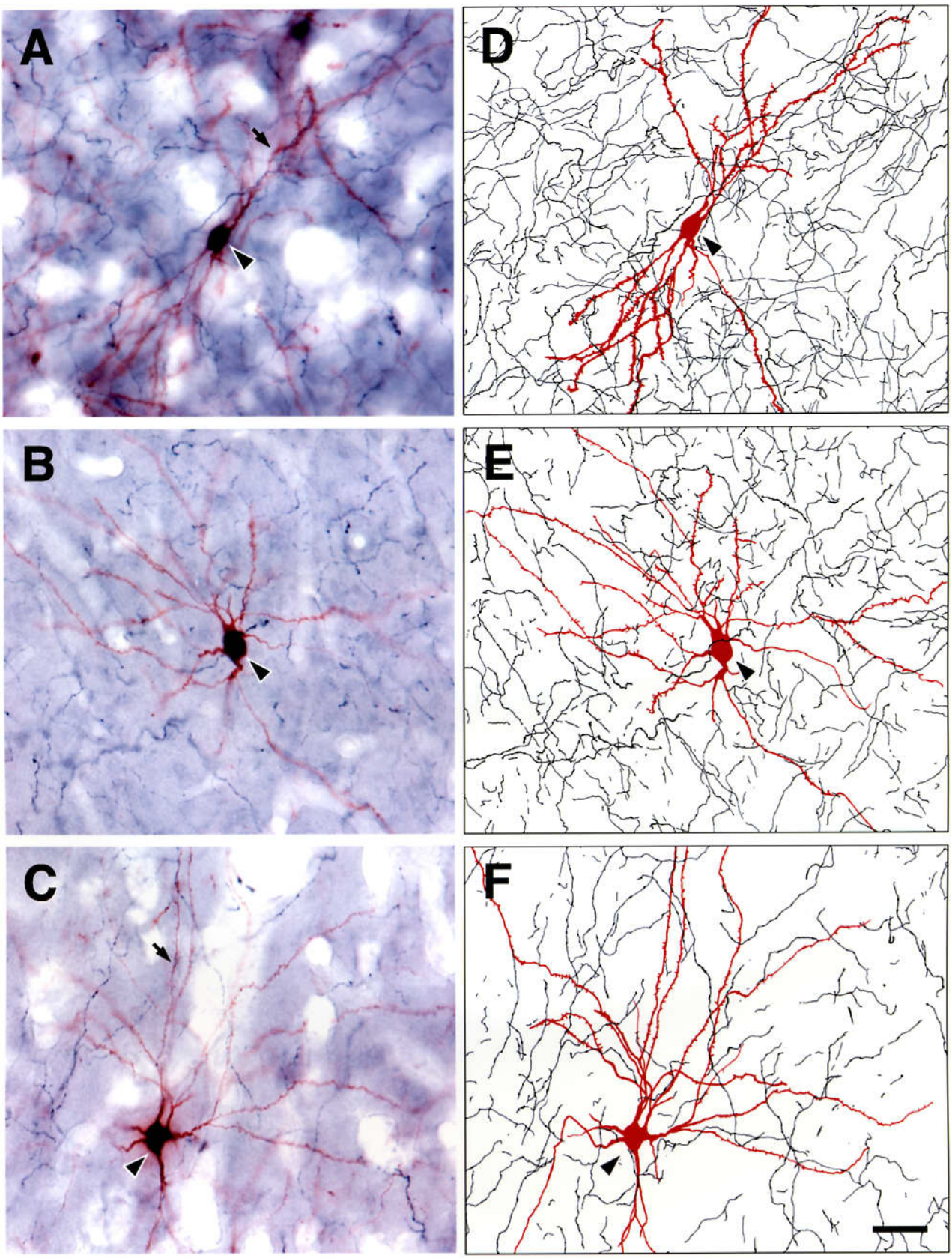
A
B
C
D
E
F

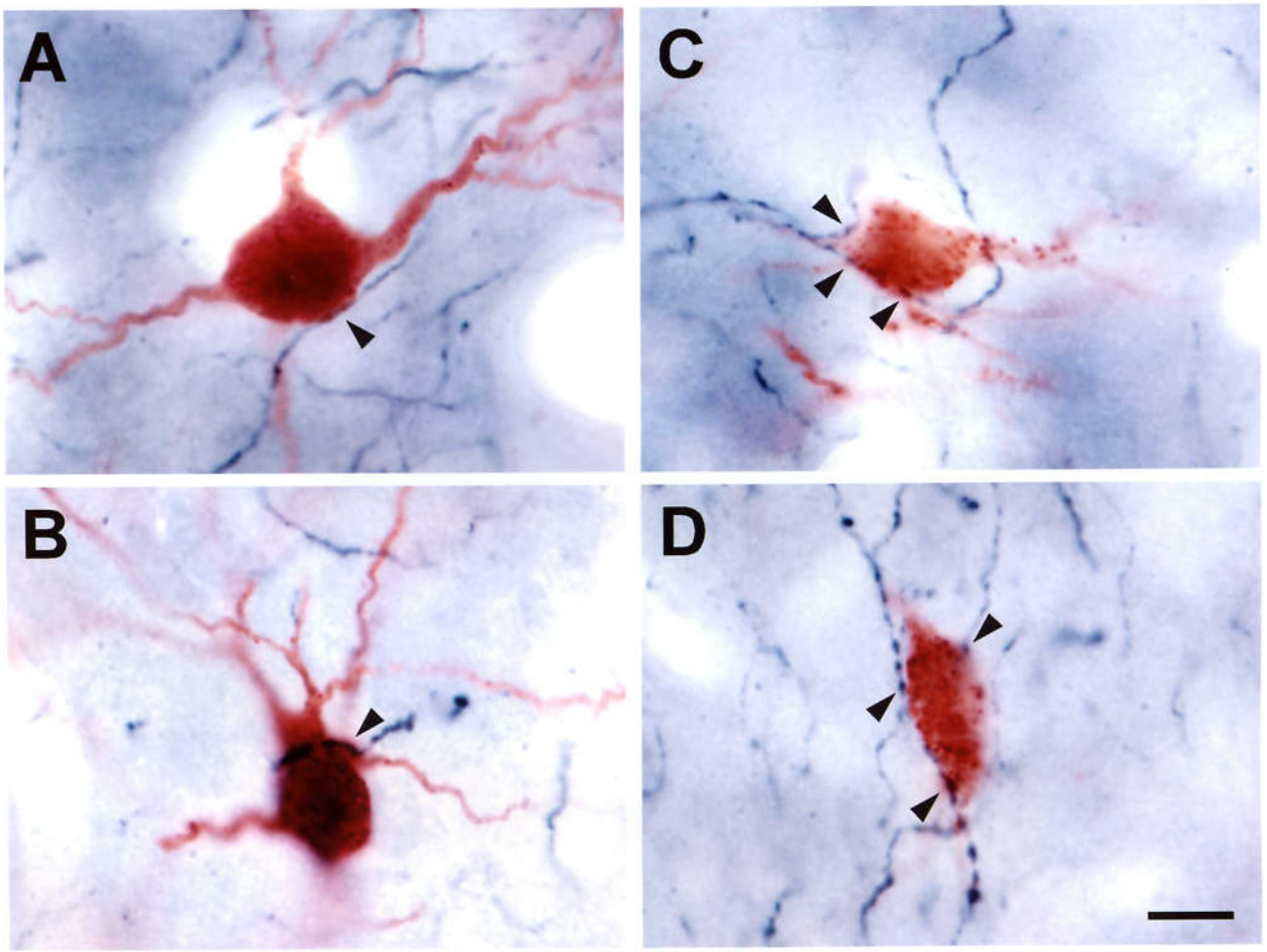
A
C
B
D

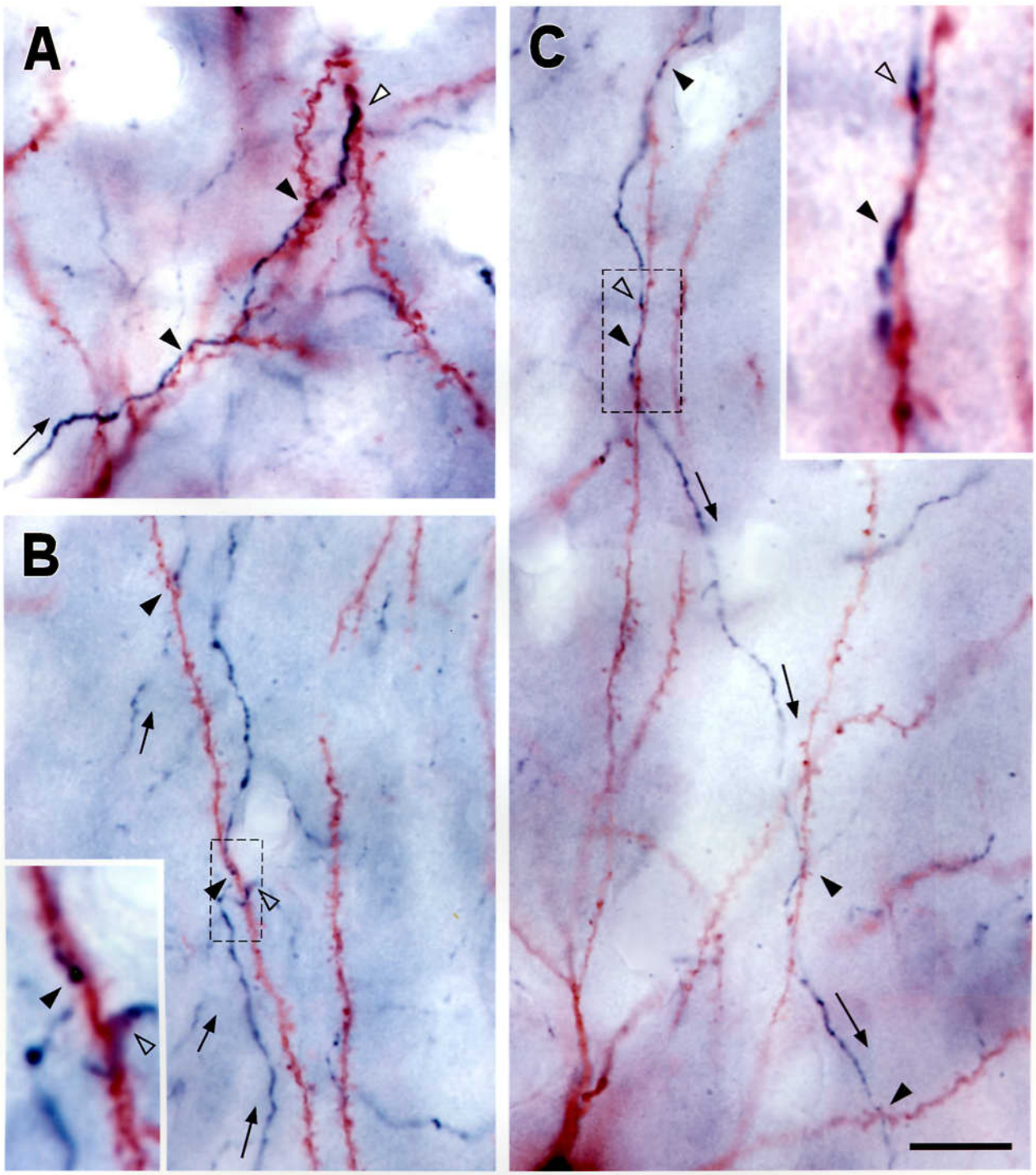
A
B
C

Figure 9 Okumura *et al.*

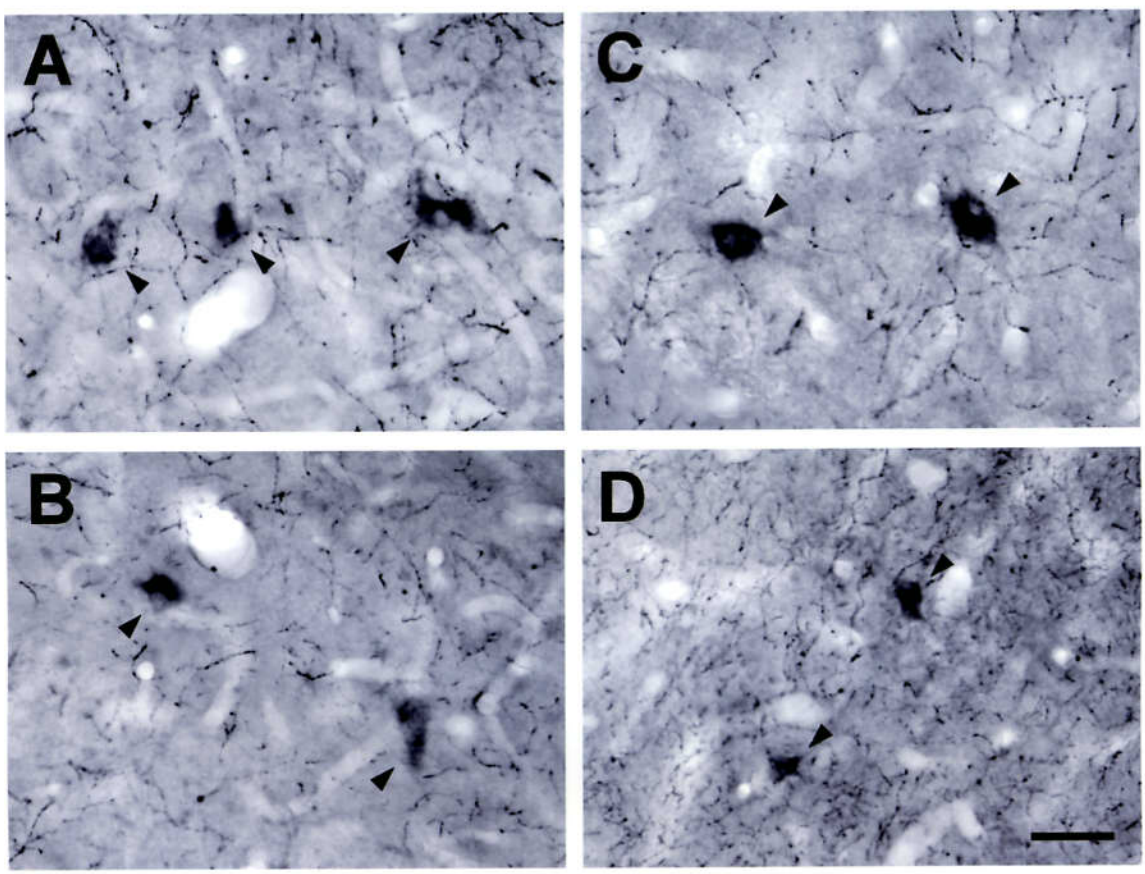

Figure 10

Okumura *et al.*

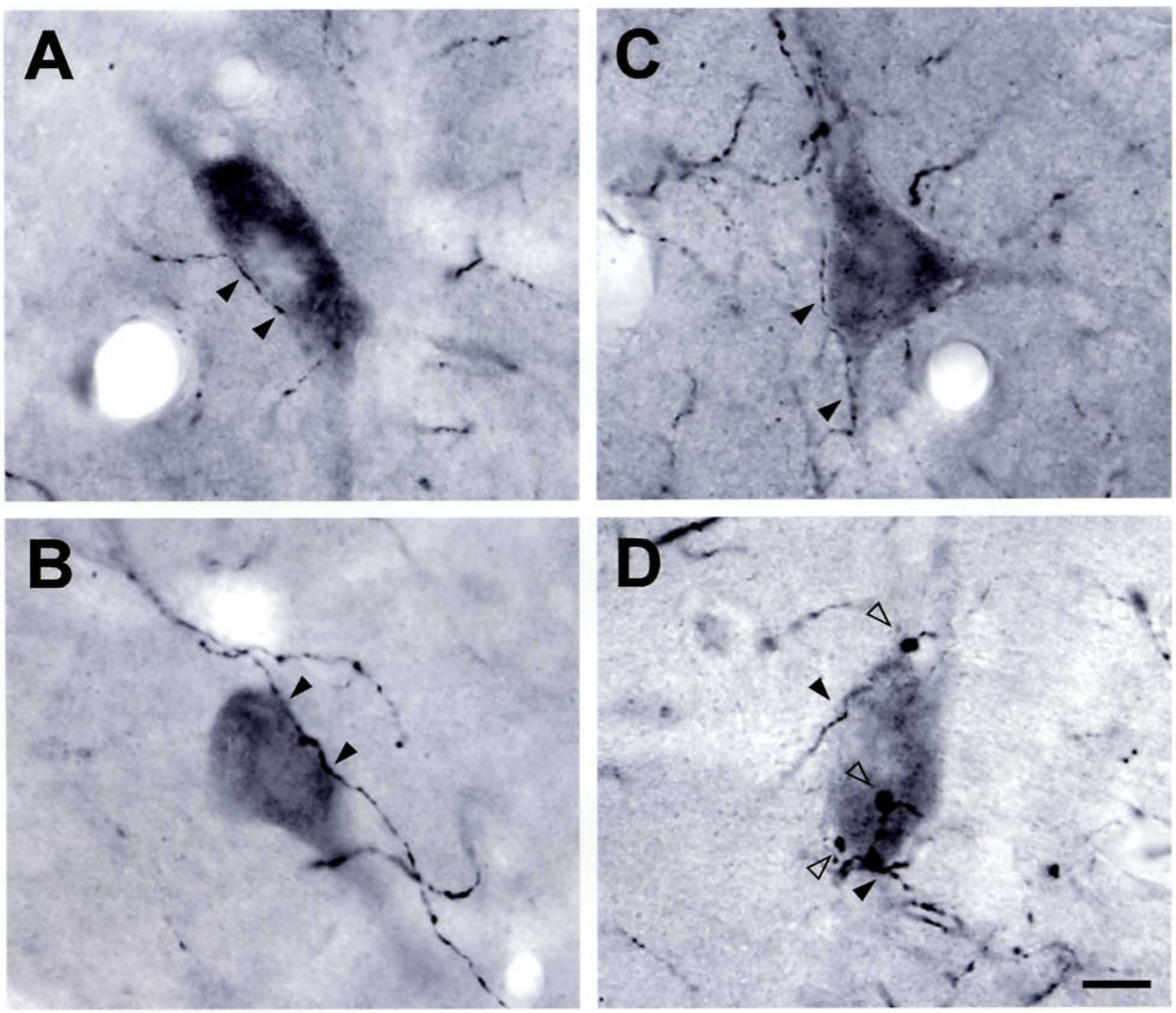

ACKNOWLEDGEMENTS

I would like first of all to thank to Professor S. Mori for his teachings and for the encouragement in preparing the doctoral dissertation. I owe a special debt of gratitude to his tireless supports and advices.

I also would like to express my sincere gratitude to Associate Professor K. Matsuyama, who initiated me into the field of neuroanatomy and neurophysiology. He generously taught me not only how to make good sections, but also how to analyze and present them in the best way.

I would like to thank all the colleagues in the laboratory, and especially to Drs. F. Mori, A. Dobolyi and B Kuze, for their valuable scientific comments and continuous supports.

Thanks also to Dr. D. G. Stuart, Regent Professor, Department of Physiology, The University of Arizona College of Medicine, for fruitful discussion, critically reviewing and editing this manuscript.

I am very grateful to Dr. H. Kimura, Shiga University of Medical Sciences, for his generous supply of 5-HT antibody, Dr. M. Skup, Nencki Institute of Experimental Biology in Poland, for her guidance in ChAT-immunohistochemistry technique.

I also sincerely thank to Mr. M. Mori and Ms. C. Takasu for their excellent technical assistance in photography and histology.

Finally I wish to thank my parents for many sacrifices they made to allow me to complete my education.

This study is supported by Grants in Aid for Scientific Research from the Ministry of Education, Science, Sports and Culture of Japan (06404087 to S. M. and 11170253 to K. M.)